Defense Threat Reduction Agency
8725 John J. Kingman Road, MS-6201
Fort Belvoir, VA 22060-6201

DTRA-TR-15-13

TECHNICAL REPORT

A Model of Medical Countermeasures for Organophosphates

October 2015

HDTRA1-10-C-0025

Jason Rodriguez and
Gene E. McClellan

Prepared by:
Applied Research Associates, Inc.
801 N. Quincy Street
Suite 700
Arlington, VA 22203

DESTRUCTION NOTICE:

Destroy this report when it is no longer needed.
Do not return to sender.

PLEASE NOTIFY THE DEFENSE THREAT REDUCTION AGENCY, ATTN: DTRIAC/ J9STT, 8725 JOHN J. KINGMAN ROAD, MS-6201, FT BELVOIR, VA 22060-6201, IF YOUR ADDRESS IS INCORRECT, IF YOU WISH THAT IT BE DELETED FROM THE DISTRIBUTION LIST, OR IF THE ADDRESSEE IS NO LONGER EMPLOYED BY YOUR ORGANIZATION.

REPORT DOCUMENTATION PAGE

Form Approved
OMB No. 0704-0188

1. REPORT DATE *(DD-MM-YYYY)*	**2. REPORT TYPE**	**3. DATES COVERED** *(From - To)*
00-10-2015	Technical	April 15, 2010 - April 14, 2013

4. TITLE AND SUBTITLE

A Model of Medical Countermeasures for Organophosphates

5a. CONTRACT NUMBER

HDTRA-1-10-C-0025

5b. GRANT NUMBER

5c. PROGRAM ELEMENT NUMBER

6. AUTHOR(S)

Jason Rodriguez
Gene E. McClellan

5d. PROJECT NUMBER

5e. TASK NUMBER

5f. WORK UNIT NUMBER

7. PERFORMING ORGANIZATION NAME(S) AND ADDRESS(ES)

Applied Research Associates, Inc.
801 N. Quincy St.
Suite 700
Arlington, VA 22203

8. PERFORMING ORGANIZATION REPORT NUMBER

9. SPONSORING / MONITORING AGENCY NAME(S) AND ADDRESS(ES)

Defense Threat Reduction Agency
8725 John J. Kingman Road, STOP 6201
Fort Belvoir, VA 22060-6201

10. SPONSOR/MONITOR'S ACRONYM(S)

DTRA

11. SPONSOR/MONITOR'S REPORT NUMBER(S)

DTRA-TR-15-13

12. DISTRIBUTION / AVAILABILITY STATEMENT

Distribution Statement A. Approved for public release; distribution is unlimited.

13. SUPPLEMENTARY NOTES

This work was sponsored by the Defense Threat Reduction Agency.

14. ABSTRACT

This paper describes a toxicokinetic/dynamic model of inhaled, intravenous, and percutaneous exposure to several organophosphates (OPs). The model predicts the efficacy of medical countermeasures via a pharmacokinetic/dynamic model of oxime, anticholinergic, anticonvulsant, and bioscavenger treatment regimens.

15. SUBJECT TERMS

CWAs Organophosphates Pharmacokinetics Toxicodynamics Countermeasures

16. SECURITY CLASSIFICATION OF:			**17. LIMITATION OF ABSTRACT**	**18. NUMBER OF PAGES**	**19a. NAME OF RESPONSIBLE PERSON**
a. REPORT	**b. ABSTRACT**	**c. THIS PAGE**	SAR	75	Dr. Christopher Kiley
Unclassified	Unclassified	Unclassified			**19b. TELEPHONE NUMBER** *(include area code)* 703-767-3460

CONVERSION TABLE

Conversion Factors for U.S. Customary to metric (SI) units of measurement.

MULTIPLY →	BY →	TO GET
← TO GET	← BY	← DIVIDE
angstrom	1.000 000 x E -10	meters (m)
atmosphere (normal)	1.013 25 x E +2	kilo pascal (kPa)
bar	1.000 000 x E +2	kilo pascal (kPa)
barn	1.000 000 x E -28	meter^2 (m^2)
British thermal unit (thermochemical)	1.054 350 x E +3	joule (J)
calorie (thermochemical)	4.184 000	joule (J)
cal (thermochemical/cm^2)	4.184 000 x E -2	mega joule/m^2 (MJ/m^2)
curie	3.700 000 x E +1	*giga bacquerel (GBq)
degree (angle)	1.745 329 x E -2	radian (rad)
degree Fahrenheit	$t_k = (t^of + 459.67)/1.8$	degree kelvin (K)
electron volt	1.602 19 x E -19	joule (J)
erg	1.000 000 x E -7	joule (J)
erg/second	1.000 000 x E -7	watt (W)
foot	3.048 000 x E -1	meter (m)
foot-pound-force	1.355 818	joule (J)
gallon (U.S. liquid)	3.785 412 x E -3	meter^3 (m^3)
inch	2.540 000 x E -2	meter (m)
jerk	1.000 000 x E +9	joule (J)
joule/kilogram (J/kg) radiation dose absorbed	1.000 000	Gray (Gy)
kilotons	4.183	terajoules
kip (1000 lbf)	4.448 222 x E +3	newton (N)
kip/inch^2 (ksi)	6.894 757 x E +3	kilo pascal (kPa)
ktap	1.000 000 x E +2	newton-second/m^2 ($N-s/m^2$)
micron	1.000 000 x E -6	meter (m)
mil	2.540 000 x E -5	meter (m)
mile (international)	1.609 344 x E +3	meter (m)
ounce	2.834 952 x E -2	kilogram (kg)
pound-force (lbs avoirdupois)	4.448 222	newton (N)
pound-force inch	1.129 848 x E -1	newton-meter (N-m)
pound-force/inch	1.751 268 x E +2	newton/meter (N/m)
pound-force/foot^2	4.788 026 x E -2	kilo pascal (kPa)
pound-force/inch^2 (psi)	6.894 757	kilo pascal (kPa)
pound-mass (lbm avoirdupois)	4.535 924 x E -1	kilogram (kg)
pound-mass-foot^2 (moment of inertia)	4.214 011 x E -2	kilogram-meter^2 ($kg-m^2$)
pound-mass/foot^3	1.601 846 x E +1	kilogram-meter^3 (kg/m^3)
rad (radiation dose absorbed)	1.000 000 x E -2	**Gray (Gy)
roentgen	2.579 760 x E -4	coulomb/kilogram (C/kg)
shake	1.000 000 x E -8	second (s)
slug	1.459 390 x E +1	kilogram (kg)
torr (mm Hg, 0^0 C)	1.333 22 x E -1	kilo pascal (kPa)

*The bacquerel (Bq) is the SI unit of radioactivity; 1 Bq = 1 event/s.

**The Gray (GY) is the SI unit of absorbed radiation.

Table of Contents

List of Figures

List of Tables

Preface

The research and development work described in this report was conducted under subcontract for Gryphon Scientific, LLC, for the Joint Science and Technology Office (JSTO) of the Department of Defense (DoD) Chemical and Biological Defense (CBD) Program. JSTO is also the Chemical/Biological Technologies (CB) Directorate in the Research and Development (RD) Enterprise of the Defense Threat Reduction Agency (DTRA). Contract HDTRA1-10-C-0025 is titled *Medical Countermeasures for CBR Agents*.

This project was initiated by Ms. Nancy Nurthen, of the Information Systems Capability Development Division (J9-CB) and continued by Dr. Christopher Kiley. It was funded under DTRA Contract Number HDTRA1-10-C-0025 to Gryphon Scientific, LLC, with subcontractor Applied Research Associates, Inc. (ARA). The target application for the product of this contract is under the auspices of the Joint Project Manager for Information Systems (JPM IS) of the Joint Program Executive Office for Chemical and Biological Defense (JPEO-CBD).

The authors wish to thank Dr. Paul Weber of ARA, for reviewing this report and offering helpful suggestions.

Section 1.

Executive Summary

A model for medical countermeasure treatment of inhaled, intravenous, and percutaneous exposure to several organophosphates (OPs) was developed to predict the efficacy of various treatment regimens. The baseline model of OP function and the OP injury model both use a series of rate equations that predict the inhibition of acetylcholinesterase, the percentage of stimulated receptors in the body, resulting from that inhibition, and the probability of mortality associated with prolonged receptor stimulation. The treatment models include rate equations for oximes, anticholinergics, anticonvulsants, and bioscavengers. These models aid in the study of the efficacy of treatment regimens by allowing the user to specify administration time, dose, and frequency. We have provided the model framework and parameters for five organophosphates, four oximes, one anticholinergic, one anticonvulsant, and one bioscavenger. Model calculations may be used to analyze consequences of exposure to OPs and the effect of treatment, based on different treatment combinations. The model may facilitate OP treatment planning and countermeasure development by helping people understand and visualize how these treatments work. In addition, the models may be used to estimate the impact of resource-limited care on the warfighter, relative to an idealized treatment regimen.

This page is intentionally left blank.

Section 2.

Introduction

This paper presents a model for estimating the efficacy of medical countermeasures for organophosphate exposure. Organophosphate (OP) molecules target acetylcholinesterase, an essential enzyme on the post-synaptic neuron responsible for breaking down the neurotransmitter acetylcholine (ACh), thereby limiting stimulation of the muscarinic and nicotinic receptors. OP molecules bind to post-synaptic acetylcholinesterase (AChE), interfering with the breakdown of ACh and leading to overstimulation of post-synaptic receptors. At low OP exposures, the resulting overstimulation of various muscle groups leads to shortness of breath, miosis, and tremors; even higher exposures lead to convulsions, respiratory failure, and neurological effects. The model in this paper consists of a toxicokinetictoxicodynamic approach to describing normal synaptic processes and the mechanism of OP injury and a pharmacokinetic/phamacodynamic approach to describing the ameliorating effects of four medical countermeasures (MCMs). The model calculates overstimulation of post-synaptic receptors after a given OP exposure, uses a toxicodynamic model to correlate overstimulation with the probability of mortality, and calculates the efficacy of MCM treatment regimens, based on reduced mortality. This modeling framework allows us to adjust parameters for OPs and medical countermeasures, so that injury and treatment efficacy can be calculated for new OPs and new countermeasures having the same modes of action. This report presents parameters for six highly toxic OPs and four classes of medical countermeasures.

The six OPs considered here are military threats that have been developed for and, in some cases, have been used in wartime situations and by terrorist groups. The six OPs chosen, along with some background information that describes their differences, are listed below.

1. Tabun (GA) – High volatility and low toxicity, compared to the other G-agents (USAMRICD, July 2000).
2. Sarin (GB) – The most volatile of the G-agents, thereby representing a considerable inhalation hazard and a negligible percutaneous hazard (USAMRICD, July 2000). Sarin was used in the Iran-Iraq war and was also used by the terrorist group, Aum Shinrikyo, in the Tokyo subway system (Yanagisawa, Morita, & Nakajima, 2006).
3. Soman (GD) – The GD/acetylcholinesterase complex forms an irreversible bond, very rapidly (approximately 2 minutes) and is thereby not affected by post-exposure antidote via oximes (USAMRICD, July 2000).
4. Cyclosarin (GF) – The least volatile of the G-agents and the most toxic, thereby representing a considerable inhalation hazard and a percutaneous hazard (USAMRICD, July 2000).
5. Nerve Agent VX (VX) – A highly toxic OP with low volatility. VX represents a considerable percutaneous hazard if the exposed person is not quickly decontaminated and treated with antidote (USAMRICD, July 2000). Due to the delay associated with skin absorption as opposed to lung absorption, responders generally have a larger window to treat exposed individuals. However, the high toxicity and persistence of VX would require considerable treatment to save an individual.

6. Russian VX (VR) – An OP with higher toxicity and lower volatility than VX and a faster aging time for the VR/acetylcholinesterase complex. Exposed individuals must be treated for VR poisoning shortly after exposure or will face severe effects and likely death.

The model captures the parameters necessary for measuring the efficacy of four classes of OP medical countermeasures (Cannard, 2006):

1. Anticholinergics – MCMs that block the binding of acetylcholinesterase (AChE) to the muscarinic receptors (mAChRs) found in the plasma membranes of neurons and lessen the amount of stimulation. The mAChRs control smooth muscle of several organs, including the diaphragm. Overstimulation leads to shortness of breath, following OP exposure. Atropine is a widely accepted anticholinergic for OP poisoning and is the only anticholinergic modeled for this project.
2. Oximes – MCMs that permanently cleave phosphorous from AChE, leaving re-activated AChE and a phosphorylated oxime. Oximes are antidotes for OP poisoning, but are effective only if the phosphorylated AChE has not yet aged, a process which forms an irreversible bond. The primary oxime currently used in the U.S. within standard issue MARK I kits is pralidoxime (2-PAM). However, due to the low efficacy of 2-PAM when used against certain OPs, this model considers three additional oximes: obidoxime, HI-6, and MMB-4.
3. Anticonvulsants – Anticonvulsants are MCMs that enhance the effect of the neurotransmitter GABA, allowing it to more rapidly bind to the GABAA receptor, resulting in central nervous system (CNS) depression and slowing the release of the neurotransmitter acetylcholine (ACh). Diazepam is the only anticonvulsant included in this model.
4. Bioscavengers (Doctor & Saxena, Bioscavengers for the Protection of Humans Against Organophosphate Toxicity, 2005) – A pretreatment/prophylaxis that sequesters highly toxic OPs before they reach their physiological targets. It has been shown that human serum butyrylcholinesterase (HuBChE) can protect against exposures of two to five times the median lethal dose (2-5 x LD50) of OPs.

The rest of this paper presents the models, the process used to develop the model parameters, and the model results.

Section 3.

Development Environment

The model was developed and tested in Berkeley Madonna v8.3.18. Berkeley Madonna is a differential equation solver ideal for modeling rate equations, allowing users to modify inputs and perform batch runs to test model sensitivity and response. Since the OP model is a series of rate equations designed to model the transmission and binding of acetylcholine, Berkley Madonna provides a robust environment for model development and testing.

Berkeley Madonna does not export source code into libraries that are useable in C++, Java or other production languages. Additionally, external programs cannot link into Berkeley Madonna's runtime environment. We developed a differential equation solver in C# and ported the Berkeley Madonna source code into the environment. Users can now run the software on any Windows PC and view the results in an Excel spreadsheet.

This page is intentionally left blank.

Section 4.

Baseline Synaptic Model and OP Exposure

In order to model organophosphate injury, one needs to define 1) the mechanisms for normal function at the nerve endings, 2) the mechanisms of response to organophosphate exposure, 3) the effect that the OP exposure has on the body, and 4) the natural biological repair/recovery mechanisms of the body. These individual processes can be combined into an OP injury and recovery model as described in this section.

4.1 Normal ACh and AChE Function in the Synapses

Figure 4-1 illustrates the normal function at the synapses of neuromuscular junctions in the absence of OP nerve agent effects. The continual cycling of choline molecules mediated by the mitochondria and acetylcholinesterase is essential to proper functioning of the synapse, enabling both voluntary and autonomic muscle control. The network of processes illustrated in Figure 4-1 is the system targeted by OPs.

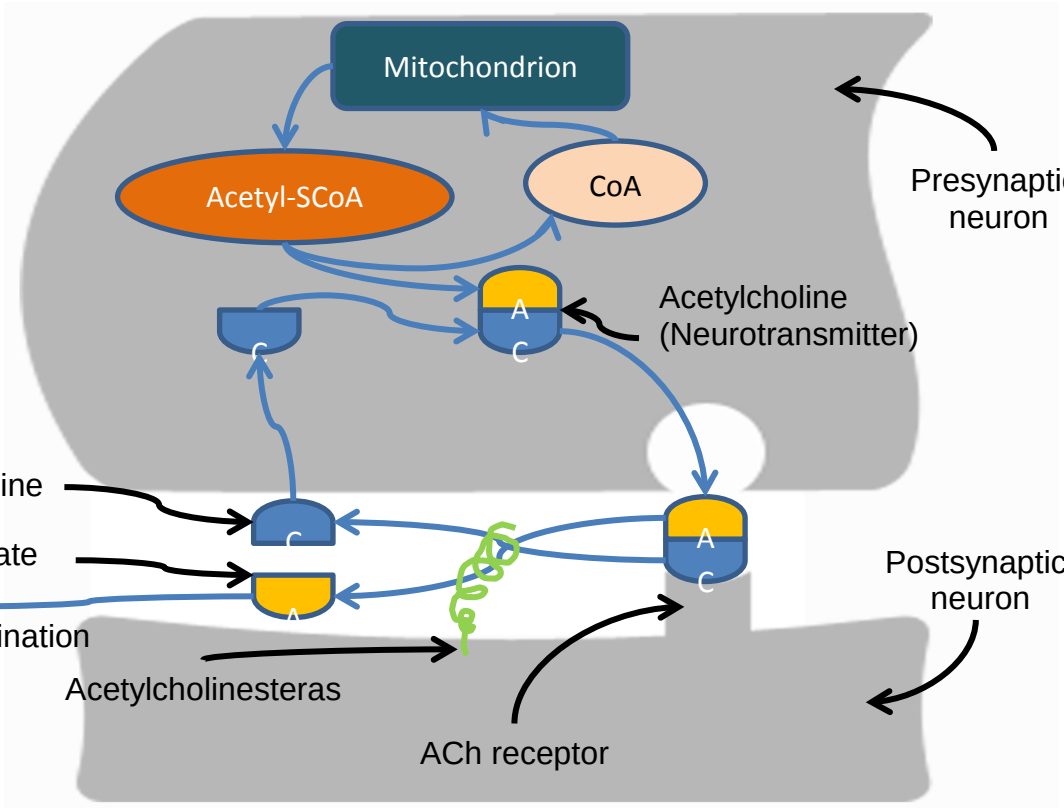

Figure 4-1. Processes for Normal Acetylcholine Function in the Synapse

As Figure 4-1 shows, ACh is created in the presynaptic neuron and binds with either the muscarinic or nicotinic receptors in the membrane of the postsynaptic nerve. Nicotinic receptors

are found at the neuromuscular junctions of skeletal muscles, at the post-ganglionic neurons of the parasympathetic nervous system, and at many different brain neurons. These sites are responsible for skeletal muscle contractions. The muscarinic receptors are found at the neuromuscular junctions of the cardiac and smooth muscles, the neuromuscular junctions of glands, and at the post-ganglionic neurons of the sympathetic nervous system. These sites control glandular activity, the smooth muscle of the respiratory and gastrointestinal system, and the efferent innervations of the heart (Weinbroum, 2004). Figure 4-2 summarizes the roles of the muscarinic and nicotinic ACh receptors. Interference of organophosphates with these functions leads directly to the signs and symptoms of nerve agent toxicity.

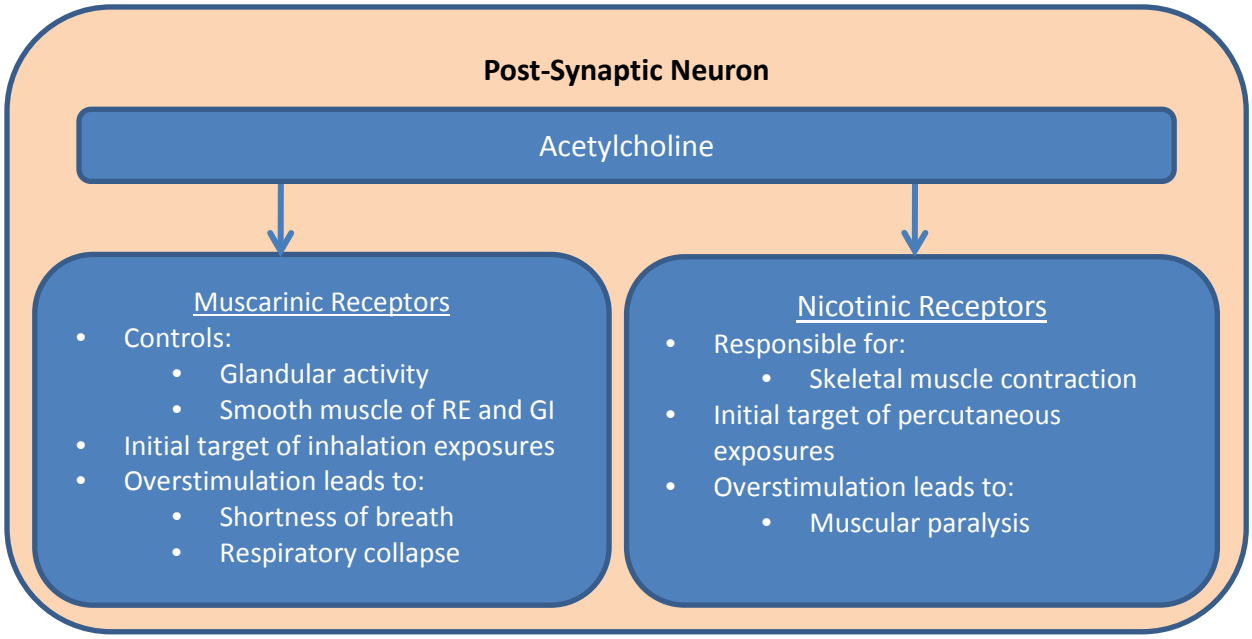

Figure 4-2. Function of ACh Receptors

AChE binds with ACh and breaks it into choline and acetate. The choline molecules are recycled by the presynaptic neuron to create new ACh molecules. The equations that describe the baseline (normal) function of ACh, AChE, and the receptors are:

$$\frac{d}{dt}R_s = k_{bind}[N] * R_f - k_{work}E * R_s$$

$$\frac{d}{dt}R_f = k_{work}E * R_s - k_{bind}[N] * R_f,$$

$$\frac{d}{dt}E = K_{syn} - k_{\deg} * E,$$

$$[N] = N_0 = K_{release}, \text{ and}$$

$$R_s + R_f = 1.$$

where:

R_s is the stimulated receptor fraction (dimensionless)

R_f is the free receptor fraction (dimensionless)

E *is* acetylcholinesterase activity (dimensionless)

[N] is the concentration of acetylcholine at the synapse (μM)

E_0 is the initial AChE activity

N_0 is the initial ACh concentration (μM)

k_{bind} is the rate of ACh binding to the free receptors (μM^{-1} min^{-1})

k_{work} is the rate of acetylcholinesterase freeing of the stimulated receptors (min^{-1})

$K_{release}$ is the concentration of acetylcholine released from the post-synaptic receptor (μM)

K_{syn} is the natural rate new AChE is produced (min^{-1})

K_{deg} is the natural rate of AChE degradation (min^{-1})

R_s is the stimulated receptor fraction and one of the primary outputs of the model. R_s and R_f define what portion of the body's total receptors are stimulated and free, respectively. These values vary rapidly on the time scale of nerve impulses; however, we take both values to be averaged over this time scale and constant under normal, healthy conditions. In our model, with unperturbed, normal functioning, we take the average values of R_s and R_f to be equal at 0.5, meaning that half of the body's receptors are stimulated and half are free. In a system perturbed by an organophosphate, the stimulated receptor fraction will increase while the free receptor fraction will decrease. This mechanism is captured by an organophosphate inhibiting E and thus, decreasing the AChE activity. The condition that $R_s + R_f = 1$ guarantees that stimulated receptor fraction will never go above one, even in a perturbed system. Later in the paper we will introduce the term R_b, which represents a free receptor that was bound by an anti-cholinergic, but not stimulated by an ACh molecule. In that case, $R_s + R_f + R_b = 1$.

E is the activity of AChE and in an unperturbed system is defined by rate of natural production of AChE (K_{syn}) minus the rate of natural degradation of AChE (k_{deg}). Our initial condition assumes K_{syn} and k_{deg} are equal, so in the unperturbed system of a healthy individual all acetylcholinesterase in the body is capable of breaking acetylcholine into acetate and choline. We used a study of AChE regeneration following inhibition of soman (*in vitro*) to estimate values for K_{syn} and k_{deg} , with both equal to 0.001 (Lanks, Dorwin, & Papirmeister, 1974). When we later introduce OP injury into the equations, the value for E will decrease with increasing OP, meaning that the acetylcholinesterase activity will decrease towards 0. If E reaches 0.5, only half of the acetylcholine will be cleaved from post-synaptic receptors. If E reaches 0, no acetylcholine will be cleaved from post-synaptic receptors. As E approaches 0, the stimulated receptor fraction will increase to one because the term $k_{work}*E*R_s$ will go to 0.

[N] is the concentration of ACh and has a normal value of $K_{release}$. $K_{release}$ is the maintained concentration of ACh in the synapse. For our model to achieve equilibrium, we set the product of k_{bind} and $K_{release}$ to k_{work}- the rate at which one molecule of AChE breaks down ACh. This makes intuitive sense, because if the product were greater than k_{work}, it would mean that the body is releasing ACh faster than the AChE could break it down. Alternatively, if k_{work} were greater than the product, it would mean that the AChE was capable of cleaving the ACh faster than it was being produced. According to the literature, one molecule of AChE is capable of degrading 25,000 molecules (4.15E-14μmol) of acetylcholine per second (2.4E-12μmol/min) (Narouzi, 2010). Since we need [N] in μM, we can divide 2.4E-12μmol/min by 2.75L, the volume of

plasma in a 70-kg man, to get 9.1E-13μM as the constant concentration of ACh in the body for an unperturbed system. We are assuming that the value remains constant even during OP injury, which implies that any ACh that cannot find a free receptor does not remain in the synapse but is instead cleared from the body. However, the value can change during diazepam treatment, as diazepam depresses the CNS and slows the release of ACh. As explained above, we set k_{work} to 9.1E-13min^{-1}, meaning fully activated AChE is capable of cleaving ACh from a free receptor at the same rate that the ACh is capable of binding to that free receptor.

Figure 4-3 shows the output for the model with no OP exposure and no countermeasures. The initial value for both R_f and R_s were set to 0 and 1, respectively. The figure shows that both R_f and R_s go to 0.5 and E stays constant at 1. We refer to these values as the baseline response.

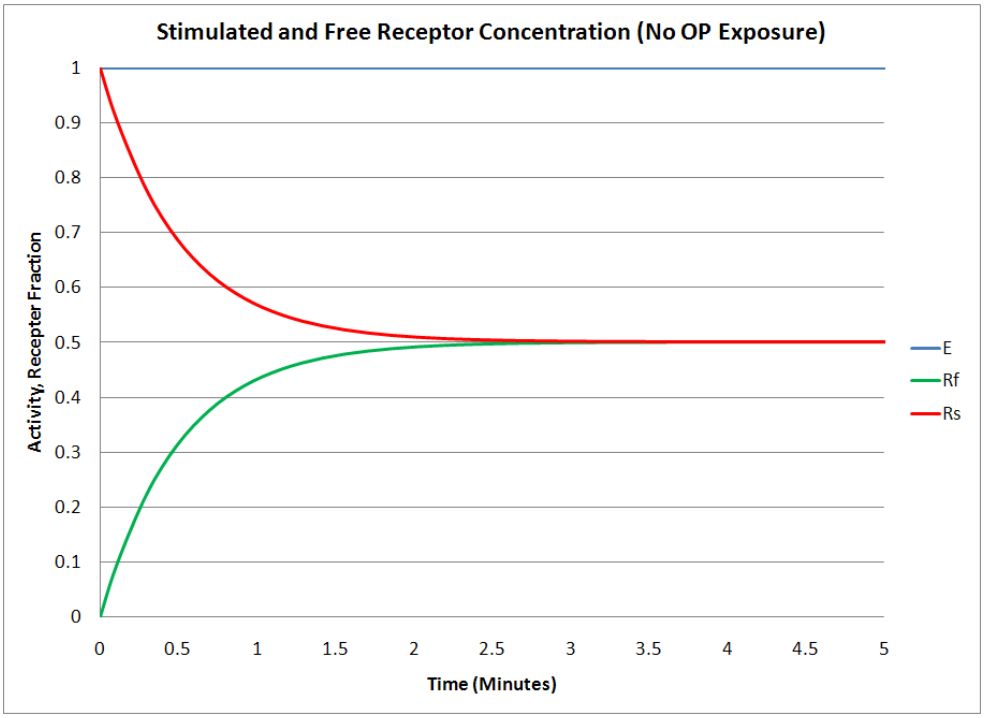

Figure 4-3. Model Output for AChE Activity and Free/Stimulated Receptor Fraction with No OP Exposure

4.2 Organophosphate Exposure Model

In order to model OP injury and to be able to compare output to available animal data, we modeled the route of exposure for the OP. We account for three different routes of exposure:

1. Percutaneous exposure via liquid droplets placed directly on the skin,
2. Inhalation exposure resulting from an individual breathing toxic vapor, and
3. Intravenous exposure via agent introduction directly into the blood stream.

Intravenous exposure was included primarily for animal comparisons and not for potential battlefield exposure scenarios. In the final C# implementation of the models, we did not include

intravenous as a route of exposure, but the source code was preserved in the Berkley Madonna code.

4.2.1. Percutaneous Exposure

Percutaneous exposure is the primary mode of exposure for the thicker organophosphates with low vapor pressure, like VX and VR. An agent with low vapor pressure remains in its liquid form for a prolonged time. If placed on the skin, a large quantity of the agent will seep through into the bloodstream before it evaporates. In order to model the rate at which OPs are absorbed through the skin, we relied on a simplified model of percutaneous exposure. The simplified model (van der Schans, 2003) defines OP concentration in the blood [*P*] with the following equation:

$$[\mathrm{P}] = [\mathrm{P}_0]\mathrm{e}^{-\mathrm{el}*\mathrm{t}} - [\mathrm{P}_0]\mathrm{e}^{-\mathrm{abs}*\mathrm{t}}$$

where

[*P*] is the concentration of OP in the blood (μM)

[P_0] is a normalization constant proportional to the amount of agent deposited on the skin (μM)

el is an elimination constant (min^{-1})

abs is an absorption constant (min^{-1})

The model is designed to account for a prolonged rise of [*P*] in the blood, followed by a prolonged period of elimination, resulting in the need for medical treatment that could last days. The parameters for human exposure to VX are shown in Table 4-1 (Worek F. , Eyer, Szinicz, & Thiermann, Simulation of Cholinesterease Status at Different Scenarios of Nerve Agent Exposure, 2007).

Table 4-1. Sample Parameters for Percutaneous VX Exposure in Humans

	1xLD$_{50}$	**3xLD$_{50}$**	**5xLD$_{50}$**
[P_0](μM)	4.784E-3	14.35E-3	23.92E-3
***abs* (min^{-1})**		0.005005	
***el* (min^{-1})**		0.003375	

The model prediction for VX concentration in the blood following 1xLD$_{50}$, administered percutaneously, is shown in Figure 4-4. As shown, it takes close to 2000 minutes for all of the VX to distribute into the body.

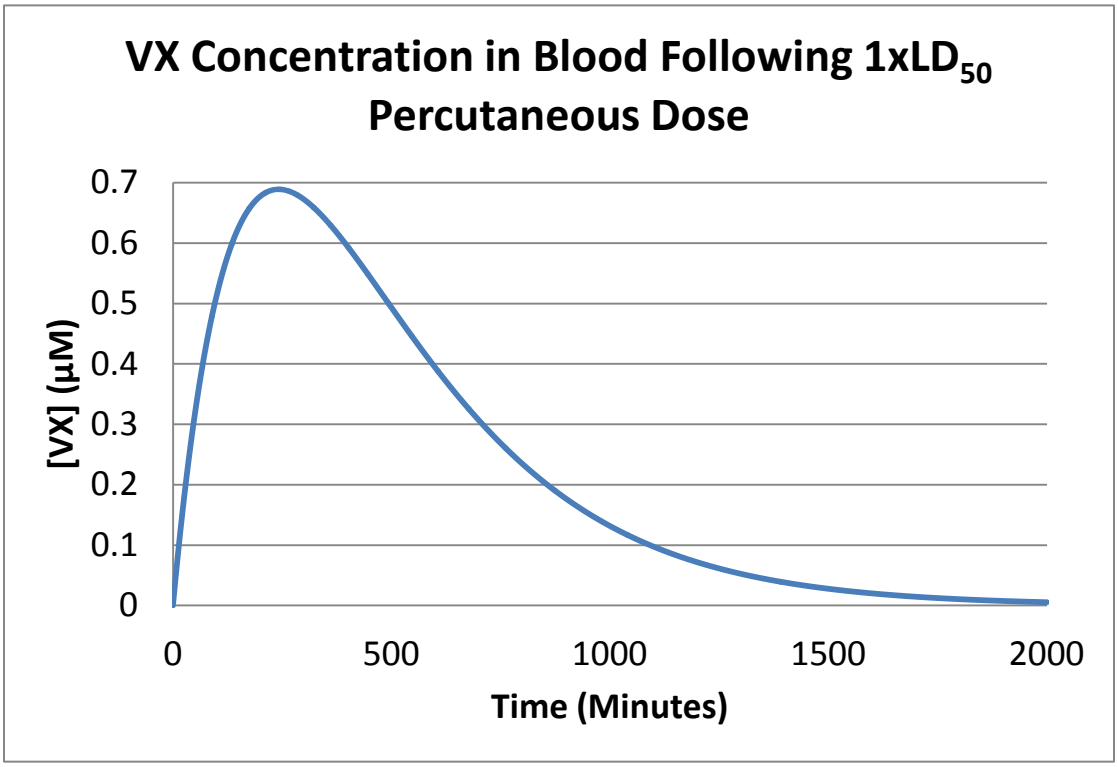

Figure 4-4. Model Prediction for VX Concentration Following 1xLD$_{50}$ Administered Percutaneously

4.2.2. Intravenous Exposure

Although not operationally important, we included an intravenous model, since many animal studies are done via intravenous exposure. We used the following toxicokinetic equation (Benschop, 2001) to calculate the concentration of OP in the blood:

$$[\mathrm{P}] = \mathrm{LD}_{\mathrm{scale}} * (\mathrm{Ae}^{-\mathrm{at}} + \mathrm{Be}^{-\mathrm{bt}} + \mathrm{Ce}^{-\mathrm{ct}})$$

where LD_{scale} is a scaling factor that allows us to model multiples of the LD$_{50}$. Each of the three terms on the right hand side of this equation represents a portion of the injected dose that is cleared at a different rate. Table 4-2 shows sample parameters for these three terms taken from the indicated references.

Table 4-2. Sample Values for Intravenous Exposure Parameters

	Soman (1xLD$_{50}$) (Benschop, 2001)	Tabun (1xLD$_{50}$) (Benschop, 2001)	Sarin (4xLD$_{50}$) (Spruit, 2000)
A **(nM)**	167.4	1564.22	1281
B **(nM)**	27.2	164.65	3.21
C **(nM)**	4.9	10.43	N/A
a **(min^{-1})**	2.2	3	4.6
b **(min^{-1})**	0.35	0.22	0.012
c **(min^{-1})**	0.073	0.047	N/A

Figure 4-5 shows the model predictions for GB concentration in the blood following exposure to 0.5, 1, and 1.5xLD$_{50}$. As shown in the graph below, an intravenous exposure results in complete removal of the agent in under a minute, mostly by binding to available AChE. The GB/AChE complex has a rate of spontaneous reactivation (Section 5.1.1) of 0, meaning that once GB binds to AChE the bond will not be broken unless it is reactivated by an oxime. Otherwise, the complex ages to an irreversible state.

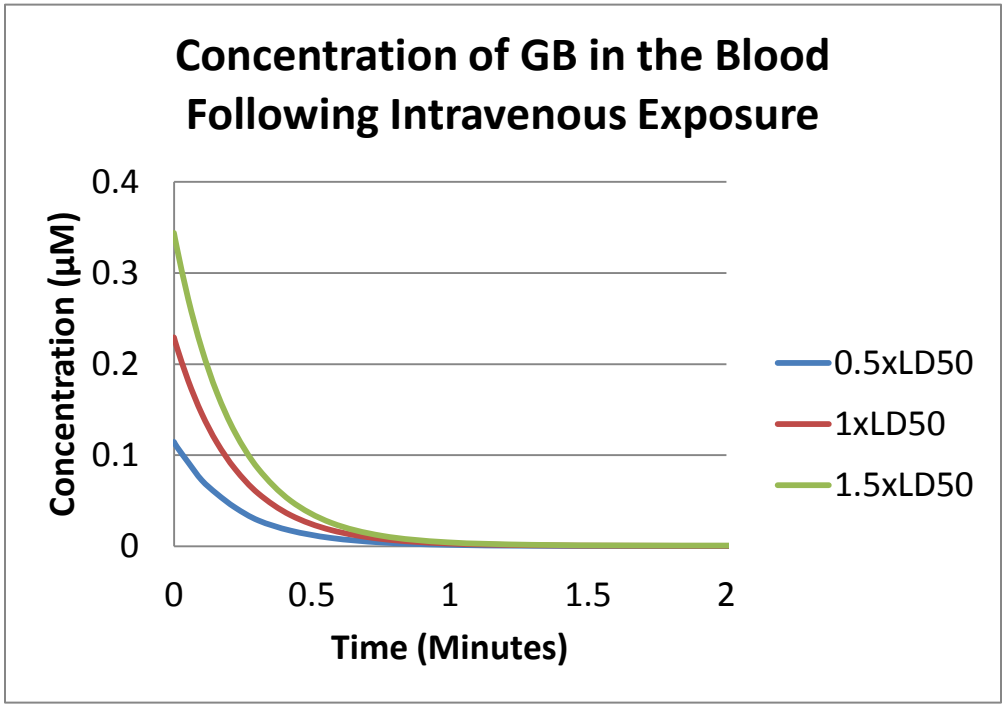

Figure 4-5. Model Prediction for GB Concentration Following Intravenous Exposure

4.2.3. Inhalation Exposure

We include a simplified exposure model in our present work with Berkeley Madonna. The inhalation equation allows the user to define the mean inhaled vapor concentration *C* in mg/m^3 over an exposure period of duration *T* in minutes. The equation that determines the resulting OP concentration in the blood as a function of time is:

$$\frac{\mathrm{d}}{\mathrm{dt}}[\mathrm{P}] = \mathrm{C(t)} *. \frac{0.015}{\mathrm{W} * \mathrm{V}} - \mathrm{k_i} * \mathrm{E} * [\mathrm{P}] - \mathrm{k_{clear}}[\mathrm{P}],$$

where

C(t) is the concentration of an agent over time (mg/m^3),

W is the molecular weight of the agent,

0.015 m^3/min is the average breathing rate for a human at rest,

V = 2.75 liters is the plasma volume for a normal, 70kg human,

k_i is the inhibition rate and is discussed in detail in Section 5.1.1 (min^{-1}μM^{-1}), and

k_{clear} is the clearance rate of unbound OP from the body (μM/min).

The resulting molar concentration [*P*] of organophosphate, once again, has units of μM. The molecular weights for the OPs included in the inhalation model are shown in Table 4-3.

Table 4-3. Molecular Weights for OPs Included in Inhalation Model

Sarin	VX	Tabun	Soman
140 g/mol	267.37 g/mol	163.13 g/mol	182.17 g/mol

For the inhalation model, we needed to include the two sink terms that represented the OP binding with the available AChE and the clearance of the remaining OP from the body. These terms were necessary because, unlike the percutaneous and intravenous model, this simplified inhalation model is not based on a toxicokinetic study and fit to measured blood concentrations of OP. The inhibition rate is discussed in Section 5.1.1. The clearance rate for sarin and tabun are equivalent to the clearance rates used in the intravenous model (0.12 and 0.047 min^{-1}, respectively). However, for soman we did not use the value from the intravenous model (0.073 min^{-1}). As we will describe in 5.1.2, the soman inhalation LCt_{50} was the only exposure route that did not produce a 50% probability of mortality for our model, if we used 0.073 min^{-1} as the clearance rate. Since the values in the table above are from pig toxicokinetic studies scaled to human parameters, we fit soman to our probability of mortality model, resulting in a lower clearance rate of 0.00175 min^{-1}.

Figure 4-6 shows the model prediction for GB concentration in the blood following a 33 mg/m^3 exposure for 1 minute, a 3.3 mg/m^3 exposure for 10 minutes, and a 0.33 mg/m^3 exposure for 100 minutes. For the 1 and 10 minute exposures, it is seen that the GB concentrations begin to overlay each other after 10 minutes. Overlays in GB concentrations occur as the body clearance is dominating the removal of GB, because the stimulated receptor fraction sink is

saturated in both cases. For the 100 minute exposure there is never any GB in the blood, due to the fact that the amount entering the blood stream is so small that it is instantly finding available AChE. If we were not counting for protracted exposure, all of these exposures would result in an effective internal dosage of 33mg-min/m^3, which is the LCt_{50} for GB for a 2-minute exposure. However, only the 1-minute exposure causes a probability of mortality of 50%. The 10-minute exposure predicts a probability of fatality of 39% and the 100-minute exposure predicts a probability of fatality of 0%. It is important to note that all three exposures will still result in serious effects.

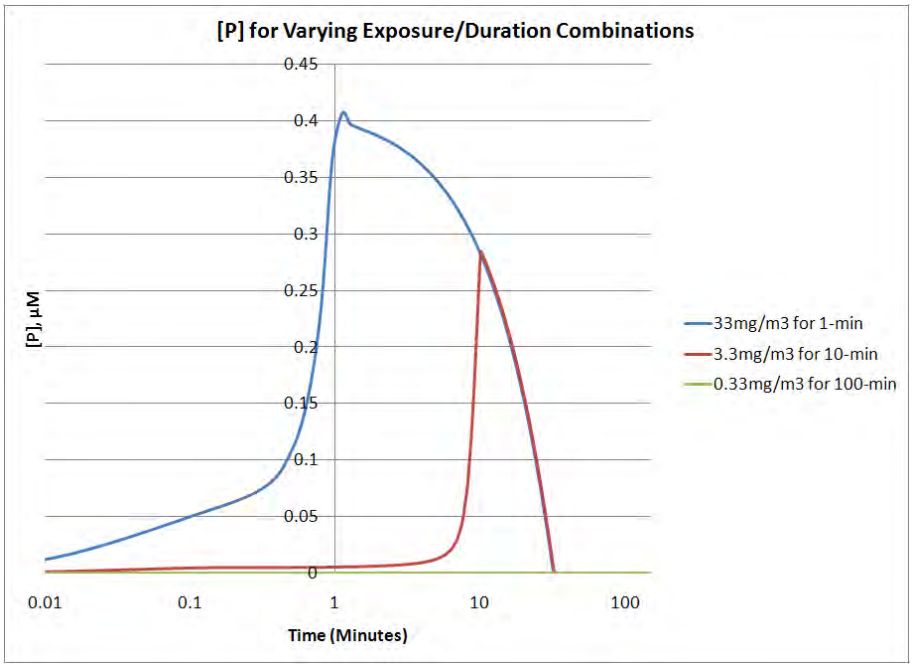

Figure 4-6. Model Prediction for GB Dosage Following Different Inhalation Exposures

4.2.4. Ingestion

Due to the fact that this model only covers battlefield injuries, ingestion is not considered.

4.3 AChE Inhibition and its Effects

Organophosphates work at the synapses by binding with AChE and inhibiting its ability to break down ACh at the receptor site. Figure 4-7 shows how OP works to inhibit AChE, thereby causing the ACh to remain bound to the postsynaptic receptor.

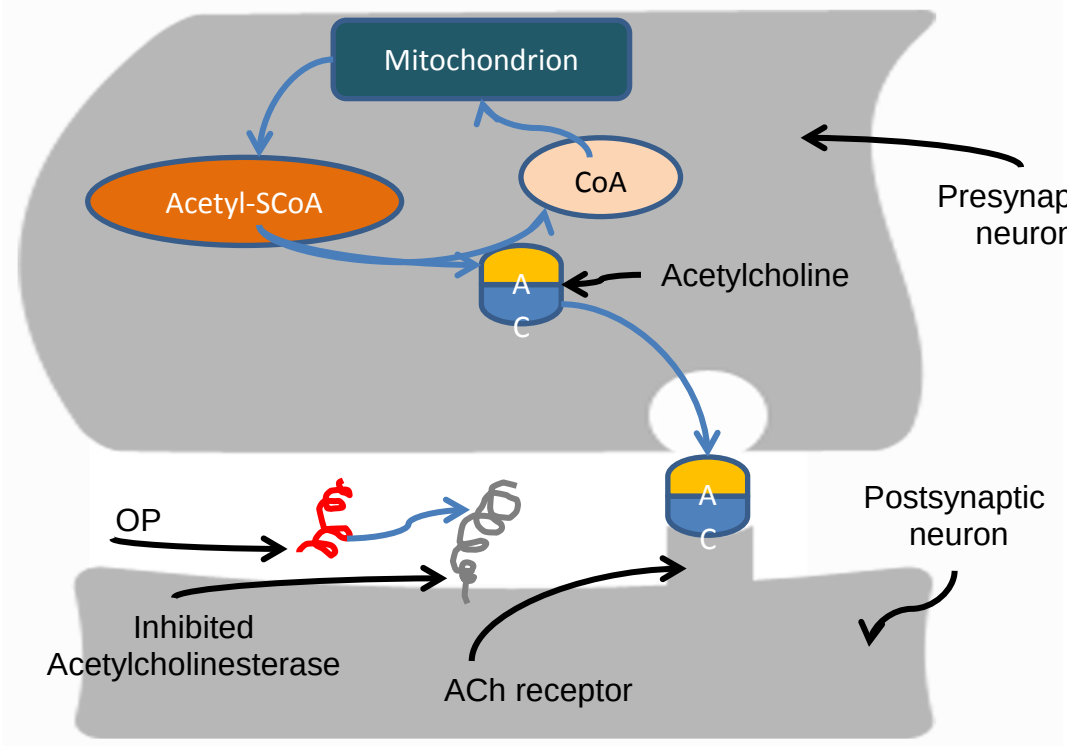

Figure 4-7. Acetylcholinesterase Inhibition at the Synapses

OP inhalation leads to rapid absorption of the agent and primarily acts on the muscarinic receptors. Severe exposure will lead to shortness of breath and complete respiratory collapse, potentially within minutes. This is the primary route of exposure for OPs with low vapor pressure, such as the G-agents. Absorption through the skin, which is common with OPs with high vapor pressure, such as VX, tends to lead to nicotinic effects at first, with severe exposures leading to complete muscular paralysis. Skin exposure will eventually lead to an accumulation of muscarinic overstimulation, thereby affecting the respiratory system and eventually causing respiratory collapse.

Once the OP binds with AChE, one of two things can happen; the AChE/OP complex can spontaneously degrade, once again activating the AChE, or the complex can age, rendering the AChE permanently inactive. The time it takes for the complex to age is agent-dependent. The soman (GD)/AChE complex, for instance, ages rapidly, rendering most post-exposure countermeasures useless.

The next section describes the OP injury and medical countermeasure model.

Section 5.

Organophosphate Injury and Medical Countermeasure Model

An overview of the model is shown in Figure 5-1.

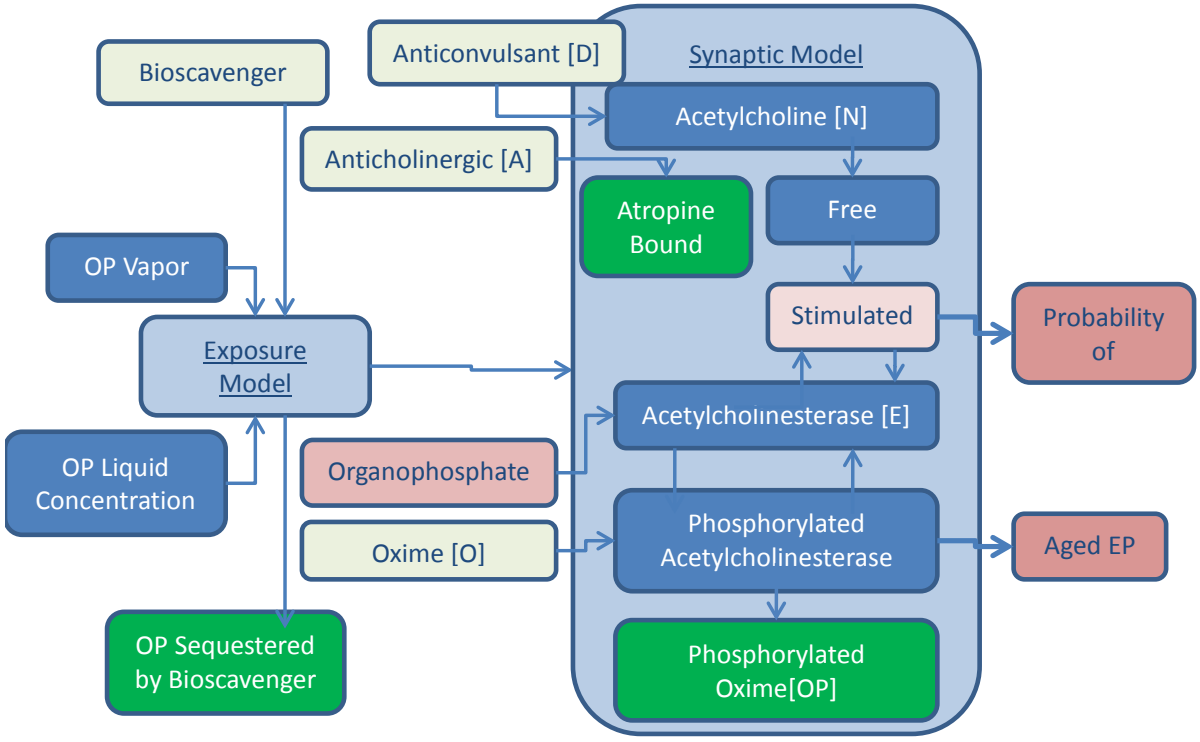

Figure 5-1. Organophosphate Injury and Medical Countermeasure Model

The model defines a series of rate equations that predict:

1. OP concentration in the bloodstream (either through inhalation, percutaneous, or intravenous exposure as described in Section 4.2),
2. The rate at which the OP inhibits the AChE, and
3. The rate of repair/competition/sequestration from the medical countermeasures included in this study.

The model structure and parameters are discussed in detail in the following sections.

5.1 Injury Model Parameters

The organophosphate injury model is shown in Figure 5-2.

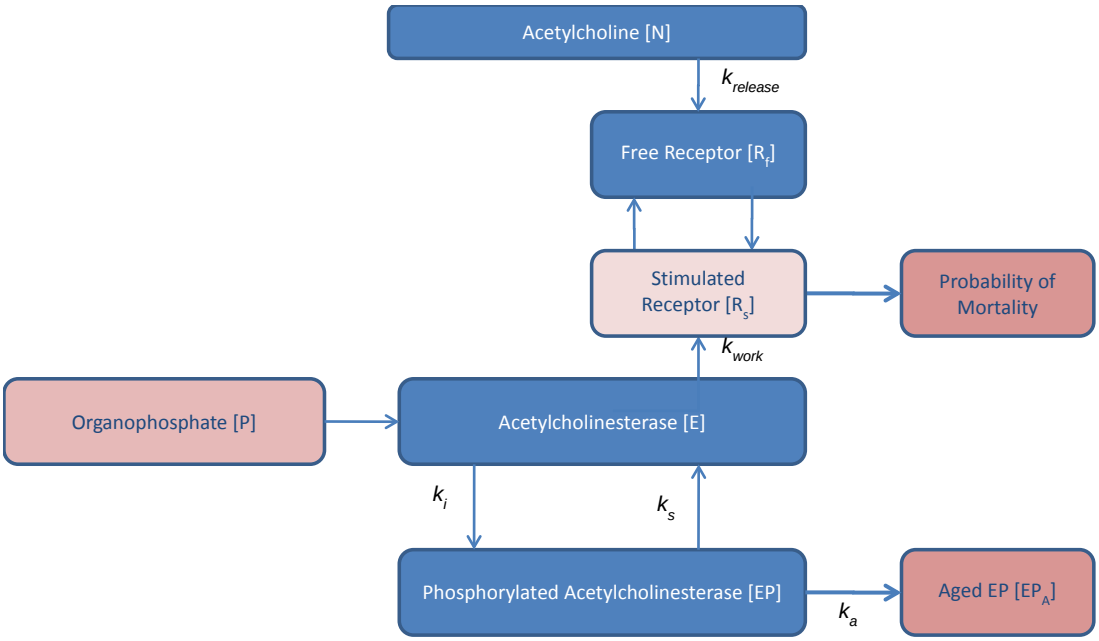

Figure 5-2. Organophosphate Injury Model

5.1.1. OP Inhibition

As mentioned in 4.1, the model estimates whole-body acetylcholinesterase activity (*E*), the stimulated receptor fraction (R_s), and free receptor fraction (R_f) by monitoring the release of ACh ([N]). For the injury model, the equations for [N], R_s, and R_f are the same as they are in the baseline model, since OP exposure has no direct effect on receptor function or acetylcholine release.

Two new terms are added to *E* for the injury model and we introduce two new compartments, the phosphorylated AChE ([EP]) and the aged AChE/OP complex ([EA]):

$$\frac{d}{dt}\mathrm{E} = -k_i * \mathrm{E} * [\mathrm{P}] + k_s * [\mathrm{EP}] + K_{syn} - k_{\mathrm{deg}} * \mathrm{E}$$

$$\frac{d}{dt}[\mathrm{EP}] = -k_a * [\mathrm{EP}] - k_s * [\mathrm{EP}] + k_i * \mathrm{E} * [\mathrm{P}]$$

$$\frac{d}{dt}[\mathrm{EA}] = k_a[\mathrm{EP}]$$

where

[EP] is the concentration of phosphorylated AChE (μM)

[EA] is the concentration of the aged AChE/OP compound (μM)

k_i is the inhibition rate ($\mu M^{-1}min^{-1}$)

k_a is the aging rate (min^{-1})

k_s is the spontaneous reactivation rate ($\mu M^{-1}min^{-1}$)

The equation for E has been modified to account for the inhibition of AChE by the OP ([P]), at rate k_i and the spontaneous reactivation of the phosphorylated AChE ([EP]) at the rate k_s. [EP] is a newly defined compartment that predicts the concentration of phosphorylated AChE by accounting for the inhibition of the AChE by the OP, the spontaneous reactivation of the phosphorylated AChE, and the aging of the phosphorylated AChE into an irreversible compound ([EA]), at a rate k_a.

The values for k_i, k_s, and k_a are all agent-dependent. Their values are reported in Table 5-1.

Table 5-1. Rate Constants for Six OPs Considered in the Injury Model

	Parameters		
	k_i (μM^{-1} min^{-1})	**k_a (min^{-1})**	**k_s (min^{-1})**
Tabun (GA) (Worek F. , Eyer, Szinicz, & Thiermann, 2007)	7.4	0.0006	0
Sarin (GB) (Worek F. , Eyer, Szinicz, & Thiermann, 2007)	2.7E1	0.0038	0
Soman (GD) (Worek F. , Eyer, Szinicz, & Thiermann, Simulation of Cholinesterease Status at Different Scenarios of Nerve Agent Exposure, 2007)	9.2E1	0.35	0
Cyclosarin (GF) (Worek, Aurbek, Wetherall, Pearce, Mann, & Thiermann, 2008)	4.84	0.00165	0
VX (Worek, Aurbek, Wetherall, Pearce, Mann, & Thiermann, 2008)	9.91E1	0.00032	0.00035
VR (Worek, Aurbek, Wetherall, Pearce, Mann, & Thiermann, 2008)	4.6E2	0.000083	0.00065

The values give us insight into the toxicity of the agents included in this model. A high k_i indicates a greater rate of AChE inhibition. For example, GA (k_i=7.4 μM^{-1} min^{-1}) would inhibit AChE at a slower rate, when compared to VX (k_i=9.91E1 μM^{-1} min^{-1}). However, the AChE in the AChE/VX complex spontaneously reactivates at a much faster rate for VX (k_s = .00035 min^{-1}) than it does in the AChE/GA complex (k_s = 0 min^{-1}). The AChE/GA complex also ages and forms an irreversible bond at twice the rate (k_a = 0.0006 min^{-1}) than the AChE/VX complex (k_s = 0.00032 min^{-1}). Also of note, soman has a very high value for k_a, which makes the AChE/GD complex age at a very fast rate that will render the complex largely unaffected by oxime treatment.

Figure 5-3 shows the model output for three different GB exposures. The individual was exposed for 1 minute to 1 mg/m^3, 12 mg/m^3, and 23 mg/m^3 resulting in dosages of 1 mg-min/m^3, 12 mg-min/m^3, and 23 mg-min/m^3, respectively. These dosages fall within the range for threshold, moderate, and severe injuries, respectively. The figure (note the log scale) shows the values for E (blue), R_f (green), and R_s (red) for each exposure. For the lowest exposure (1 mg-min/m^3, solid line), we see that E drops to approximately 0.98 and returns to the baseline after approximately 1,000 minutes. For the same exposure, the free receptor fraction drops to approximately 0.49 and the stimulated receptor fraction rises to approximately 0.51. These numbers make sense intuitively, because at this low, threshold exposure, the most significant effect is miosis, which is likely caused from percutaneous vapor exposure to the eye and would not necessarily lead to a large change in AChE activity within the body. For the highest exposure (23 mg-min/m^3, dotted line) we see that E drops to approximately 0.05 and returns to the

baseline after approximately 4,700 minutes. For the same exposure, the free receptor fraction drops to approximately 0.07 and the stimulated receptor fraction rises to approximately 0.93.

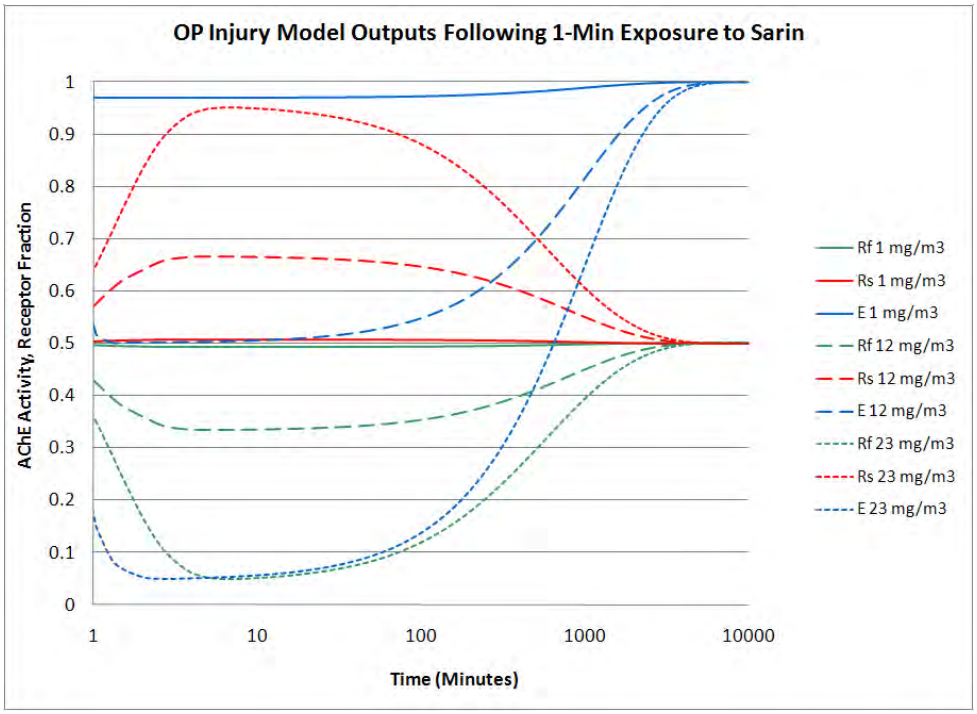

Figure 5-3. Injury Model Outputs for Three Sarin Exposures

In order to help validate the model against real-world data, we used values for k_i, k_s, and k_a for animals. These values are reported in Table 5-2.

Table 5-2. Rate Constants for Three OPs Considered in the Animal Injury Model

Animal	Parameter	GF (Worek, Aurbek, Wetherall, Pearce, Mann, & Thiermann, 2008)	VX (Aurbek, Thiermann, Szinicz, Eyer, & Worek, 2006)	VR (Aurbek, Thiermann, Szinicz, Eyer, & Worek, 2006)
Pig	k_i (μM^{-1} min^{-1})	4.84E2	4.43E1	1.88E2
	k_a (min^{-1})	0.0008	0.000135	0.000043
	k_s (min^{-1})	0	0.000143	0.000217
Mini-pig	k_i (μM^{-1} min^{-1})	4.84E2	5.61E1	1.95E2
	k_a (min^{-1})	.000717	0.00012	0.0000417
	k_s (min^{-1})	0	0.00014	0.000127

In order to compare model output for both humans and pigs and once again show the benefit of normalizing the model, we compare the model predictions for humans and mini-pigs following an intravenous exposure to GF (Figure 5-4). In both cases, the human and the pig were given doses equivalent to the human LD_{50} for GF. Since the human and mini-pig values for k_i and k_s are equivalent, and since the model is normalized to 1, we see no difference in the calculated acetylcholinesterase fraction between the two species. All AChE that becomes inhibited remains inhibited, until normal biological repair recovers the value of E to 1. However, the value for k_a is different between the two species (0.000165 min^{-1} for humans and 0.000717 min^{-1} for mini-pigs), resulting in slower aging for the mini-pig's GF/AChE complex.

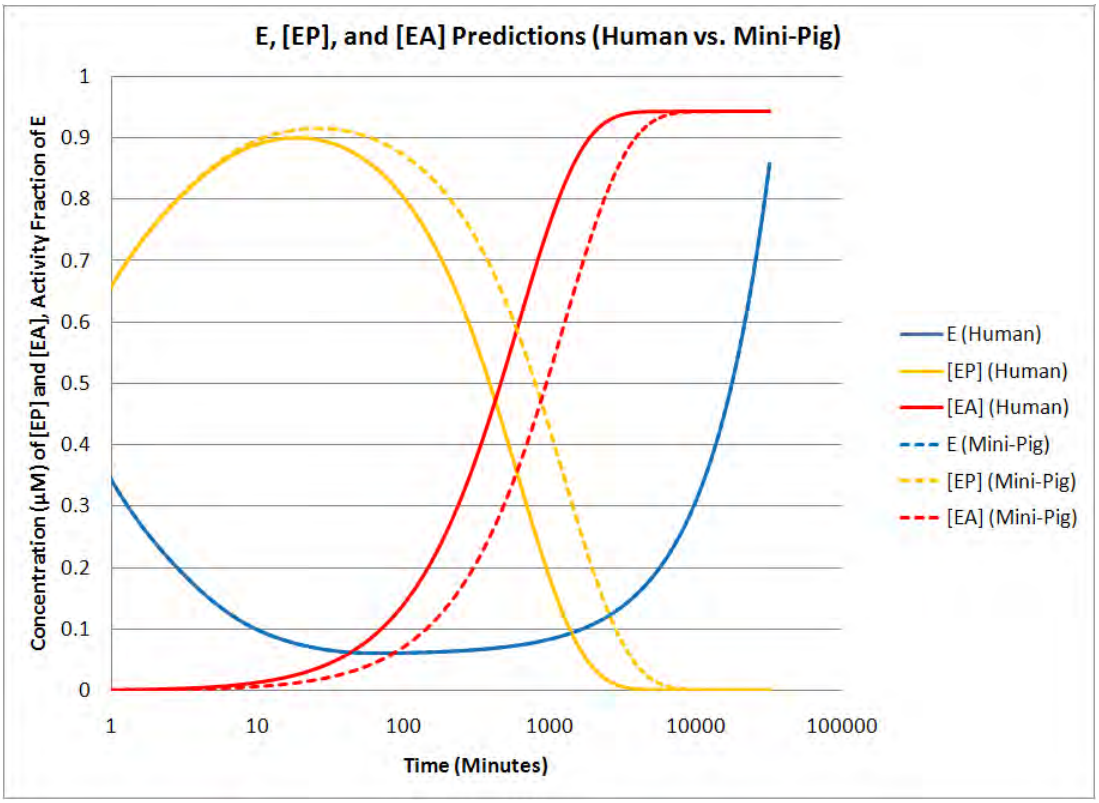

Figure 5-4. [E], [EP], and [EA] Predictions for Intravenous GF Exposure in Humans and Mini-Pigs

5.1.2. Probability of Mortality

Probability of mortality is calculated from the stimulated receptor fraction (R_s). The first step in determining probability of mortality is to ensure that different combinations of exposure routes and chemicals lead to similar stimulated receptor fractions and acetylcholinesterase fractions. Figure 5-5 shows the results of our analysis, with the LCt_{50} for inhaled sarin, the LD_{50} for intravenous sarin, Tabun, and soman, and the LD_{50} for percutaneous VX being, used as inputs into the injury model. In all cases, the AChE stimulated receptor fraction peaked at approximately 0.93. AChE Activity, a standard value used in the literature, is consistently reported to be approximately 5-10% for most LD_{50}/LCt_{50} exposures (Joosen & van der Schans, 2010). In our model, AChE Activity is approximately equal to $100*(1-R_s)$ for untreated cases.

This would mean that the maximum value we are predicting for stimulated receptor fraction corresponds to an AChE Activity of approximately 7% and is consistent with the literature.

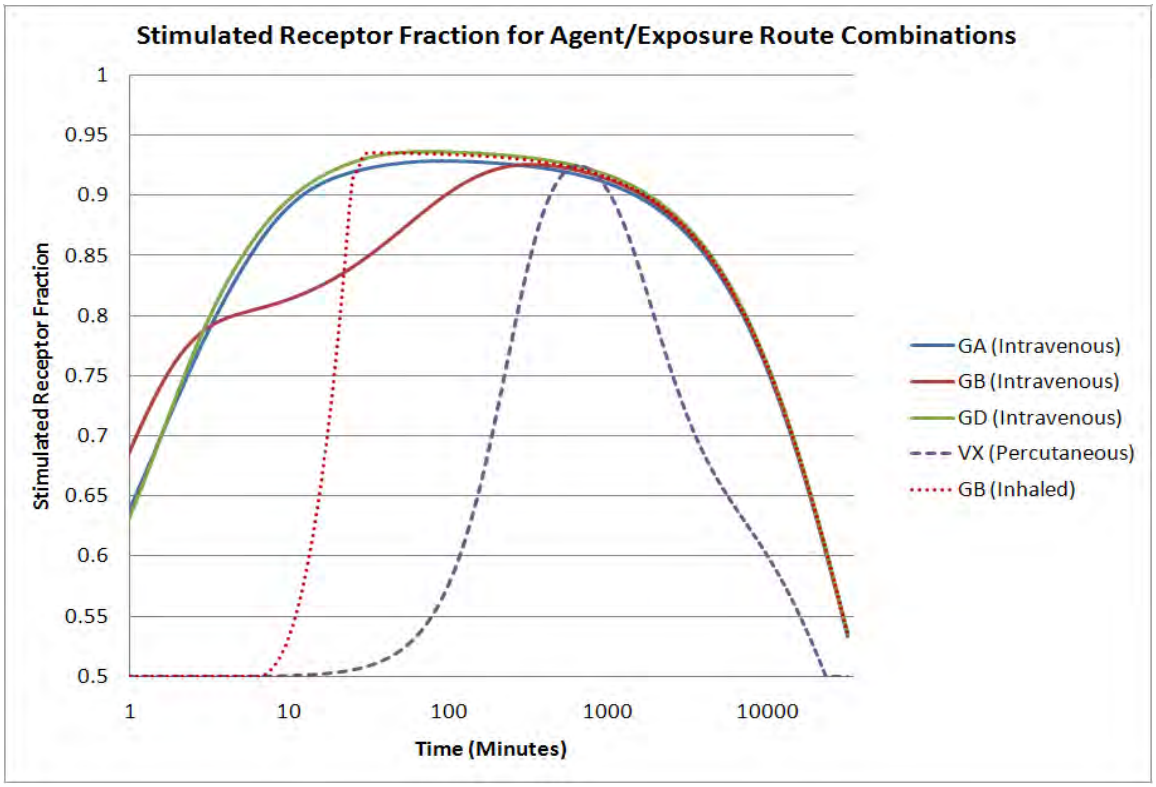

Figure 5-5. Stimulated Receptor Fractions for Five Different OP/Exposure Route Combinations

However, we cannot use the maximum value of stimulated receptors as the appropriate measure of probability of mortality. If we did, we would be neglecting the beneficial contribution of medical countermeasures that could be administered after an individual reaches the maximum stimulated receptor fraction. AMedP-8 (C) estimates a time-to-death of 30 minutes post-exposure for individuals exposed to the LCt_{50} of GB. Since oximes are capable of reversing the AChE/OP complex and therefore freeing up receptors that would have been stimulated in the absence of oxime, it is crucial to account for the duration of injury in some way in order to have an effective estimate of probability of mortality.

Our model uses a new quantity, the *time-integrated deviation* (T_{dev}). The time-integrated deviation is the area under the stimulated receptor fraction curve above the baseline stimulated receptor fraction. It is defined by:

$$\frac{d}{dt}T_{dev} = [R_s] - R_{distress}$$

where $R_{distress}$ is a constant corresponding to a value of R_s, where there is some nominal probability of fatality. Figure 5-6 shows the calculated R_s values for a range of dosages

corresponding to a GB exposure of $LCt_{0.1}$ and $LCt_{99.9}$. Note how for the $LCt_{0.1}$ exposure, the stimulated receptor fraction reaches to just over 0.8 before rapidly dropping off. This represents a very low probability of mortality (1 mortality out of every 1,000 healthy adults). For the high dosage (which represents 999 mortalities out of 1,000 people), we see that the stimulated receptor fraction saturates at 1 and remains there for close to 100 minutes. This would represent close to 100 minutes of respiratory failure and seizures. Since the model predicts a maximum R_s of 0.8 for the very low probability of mortality, we set $R_{distress}$ to 0.8.

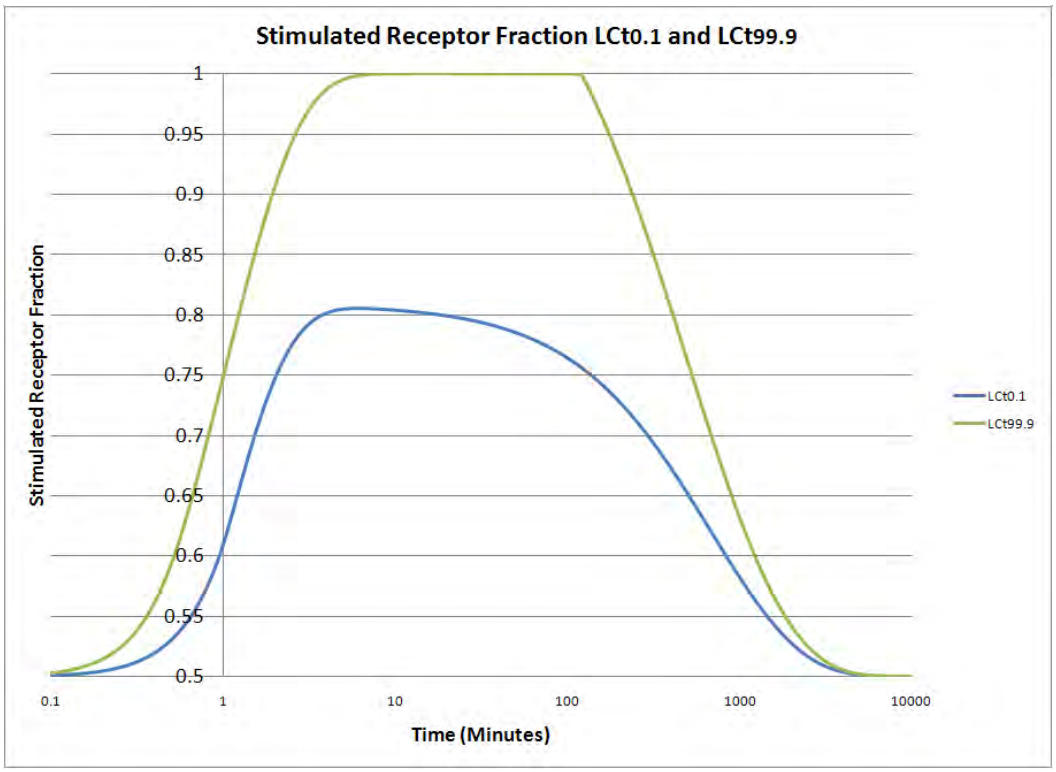

Figure 5-6. Stimulated Receptor Fractions for GB Exposure of $LCt_{0.1}$ and $LCt_{99.9}$

In order to determine probability of mortality as a function of T_{dev}, we first calculated T_{dev} for varying dosages between the $LCt_{0.1}$ and the $LCt_{99.9}$. The results are shown in Table 5-3 and plotted in Figure 5-7.

Table 5-3. T_{dev} Values for $LCt_{0.1}$-$LCt_{99.9}$

Dosage (mg-min/m^3)	Probability of Mortality (%)	T_{dev} (Minutes)
18.24	0.1	0.04
20.13	0.5	3.34
21.12	1	6.95
24.07	5	22.57
25.81	10	26.15
29	25	28.27
33	50	30.92
37.56	75	33.93
42.2	90	37
45.25	95	39.01
51.57	99	43.18
54.1	99.5	44.85
59.71	99.9	48.55

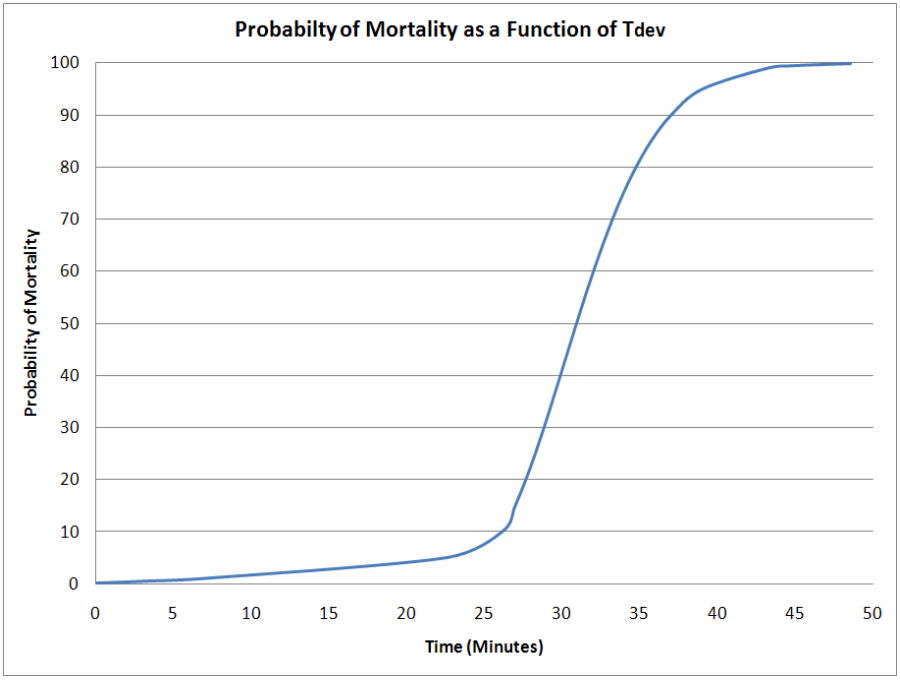

Figure 5-7. Probability of Mortality as a Function of T_{dev}

The distribution shown in Figure 5-7 can be approximated by a Laplace Distribution, due to its wide tails. We fit the CDF for the Laplace distribution

$$P = 0.5 * (1 + \mathrm{sgn}(T_{dev} - \mu) * (1 - e^{-\frac{|T_{dev} - \mu|}{b}}),$$

where

P is the probability of mortality

μ is the T_{dev} that corresponds to the LCt_{50}

b is a constant

We used Berkeley Madonna to estimate μ and *b* and obtained values of 31 and 3.9, respectively. Figure 5-8 once again shows probability of mortality as a function of T_{dev} (blue line) but with the fitted equation plotted alongside it (red line).

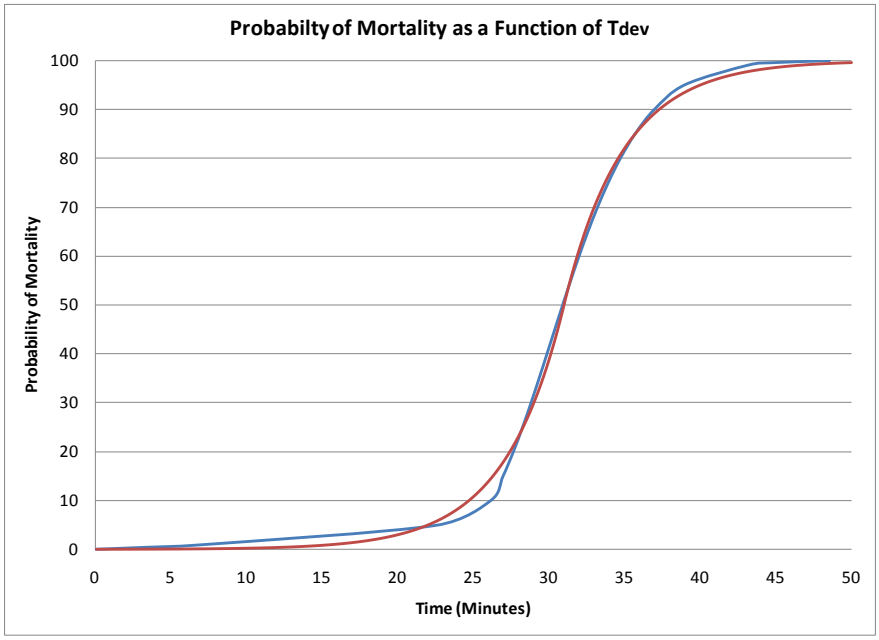

Figure 5-8. Probability of Mortality as a Function of T_{dev} with Curve Fit

One way to test the probability of mortality equation is to see how it performs with protracted exposures. We used the published Acute Exposure Guideline Levels (AEGLs) for inhaled sarin (Table 5-4) as our basis for model performance. AEGLs are a set of concentrations (in mg/m^3) defined by the Environmental Protection Agency (EPA) at which individuals might experience threshold, moderate, or severe effects (AEGLs 1, 2, and 3, respectively) after being exposed to the concentration for 10, 30, 60, 240, and 480 minutes. The AEGL values have the following definition:

1. AEGL 1 – Individuals have some chance of experiencing threshold effects
2. AEGL 2 – Individuals have some chance of experiencing moderate effects

3. AEGL 3 – Individuals have some chance of experiencing severe effects

In principle, no AEGL values should produce a probability of mortality in the model, despite the fact that an individual exposed to 0.051 mg/m^3 for 480 minutes (an AEGL 3, 8 hour) results in an internal dosage of approximately 25 mg/m^3, a severe effects-causing dosage if received over 2 minutes.

Table 5-4. AEGL Values for GB

	10 Minute (mg/m^3)	30 Minute (mg/m^3)	60 Minute (mg/m^3)	4 Hour (mg/m^3)	8 Hour (mg/m^3)
AEGL 1	0.0069	0.004	0.0028	0.0014	0.0010
AEGL 2	0.087	0.05	0.035	0.017	0.013
AEGL 3	0.38	0.19	0.13	0.07	0.051

In Table 5-5, we see that no combination of AEGL exposure and duration causes any T_{dev} probability of mortality, as expected, despite the fact that injuries are predicted.

Table 5-5. T_{dev} Calculations with a 0.8 Stimulated Receptor Fraction Threshold for GB AEGL Exposures

	10 Minute	30 Minute	60 Minute	4 Hour	8 Hour
AEGL 1	0	0	0	0	0
AEGL 2	0	0	0	0	0
AEGL 3	0	0	0	0	0

However, this result doesn't illustrate that our model is accounting for protracted exposure. To do that, we set the lower bound on the time-integrated deviation calculation to 0.5 instead of 0.8. The result can now be viewed as the T_{dev} for injury. Once again, we should expect T_{dev} to remain constant across all AEGL exposures. Table 5-6 shows the result of this simulation.

Table 5-6. T_{dev} Calculations with a 0.5 Stimulated Receptor Fraction Threshold for GB AEGL Exposures

	10 Minute	30 Minute	60 Minute	4 Hour	8 Hour
AEGL 1	0.77	0.9	0.77	0.5	0.4
AEGL 2	9.8	11.2	9.7	5.6	4.9
AEGL 3	44	44	37	23	20

It should be noted that the range for T_{dev} for injury will be much higher than the 0-50 range we saw with a threshold of 0.8 for mortality. For an exposure dosage equal to the LCt_{05} for GB, gives a T_{dev} for injury of 434 minutes compared to 22 minutes for the T_{dev} for mortality. As

shown in Table 5-6, the T_{dev} for a given AEGL does not increase with increasing duration, but rather decreases somewhat. However, the decrease is not substantial considering the scale of T_{dev} with the 0.5 threshold. We see then that the T_{dev} calculation shows sparing of effects for increasing dose protraction as expected.

5.2 Oxime Repair

5.2.1. Oxime Concentration

The concentration of oxime in the blood in the case of a needle injection is given by the following function (Worek F. , Eyer, Szinicz, & Thiermann, 2007):

$$[O] = \frac{[O_0]}{V_{DSS}} * \frac{k_{abs}}{k_{abs} - k_{el}} (e^{-k_{el}t} - e^{-k_{abs}t})$$

where

[O] is the concentration of oxime in the blood

$[O_0]$ is the administered dose

V_{DSS} is the volume of distribution of the drug (the number that quantifies the distribution of the drug in the body after administration),

k_{abs} and k_{el} are the absorption and elimination rate constants.

Values for the above equation are given in Table 5-7. The values given are for doses of the oxime used in practice. Our implementation allows the user to input the time at which the oxime was administered and the frequency of administration, for multiple doses.

Table 5-7. Sample Values for Oximes that are used to Predict Human Blood Concentrations.

Parameter	Obidoxime (Human)	HI-6 (Human)	HI-6 (Pig)
O_0 (mg)	250	500	500
O_0 (µmol)	0.70E3	1.33E3	1.33E3
V_{DSS} (ml/kg)	173 (Sidell, Groff, & Kaminskis, Toxogonin and pralidoxime: kinetic comparison after intravenous administration to man, 1972)	240 (Clement, Bailey, Madill, Tran, & Spence, 1995)	530 (Lundy, et al., 2005)
k_{abs} (min^{-1})	0.0578 (Sidell & Groff, 1972)	0.0578 (Clement, Bailey, Madill, Tran, & Spence, 1995)	0.346 (Lundy, et al., 2005)
k_{el} (min^{-1})	0.0083 (Sidell & Groff, 1972)	0.0113 (Clement, Bailey, Madill, Tran, & Spence, 1995)	0.0085 (Lundy, et al., 2005)

Figure 5-9 shows the concentration of HI-6 in the blood for one 500 mg dose given every 250 minutes starting at 10 minutes as predicted by the model.

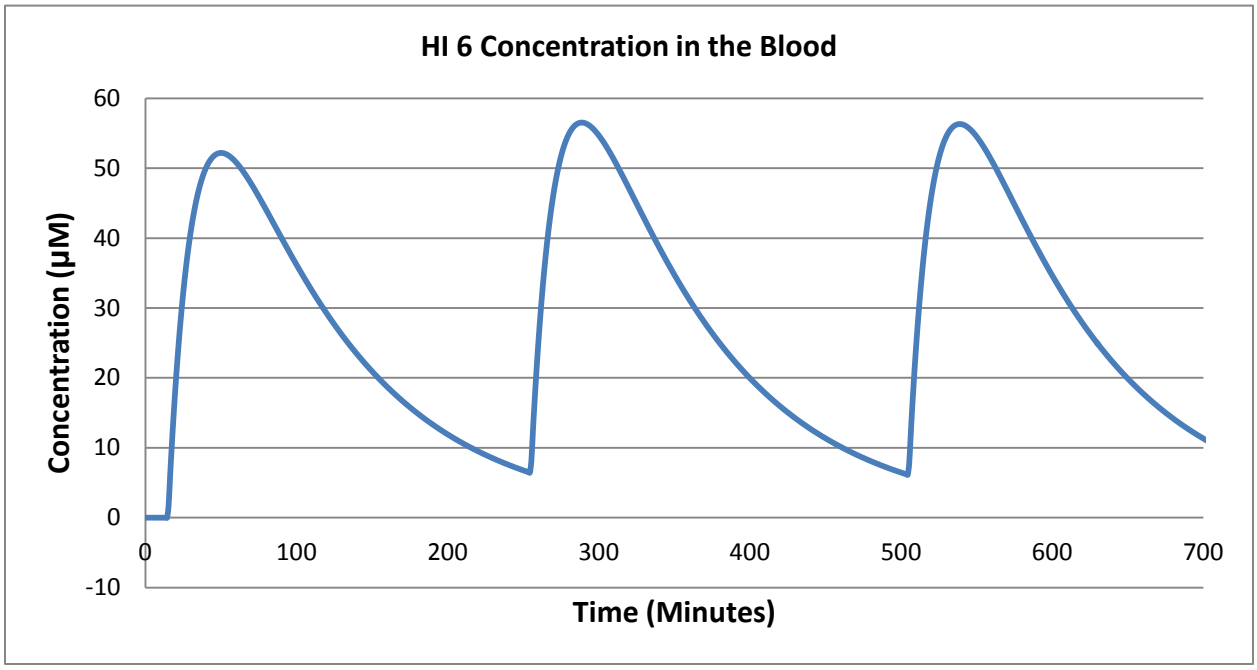

Figure 5-9. HI-6 Concentration in the Blood for a 500 mg Dose Administered every 250 Minutes, Starting at 10 Minutes Post-Exposure

5.2.2. Oxime Repair

The oxime repair model is shown in Figure 5-10.

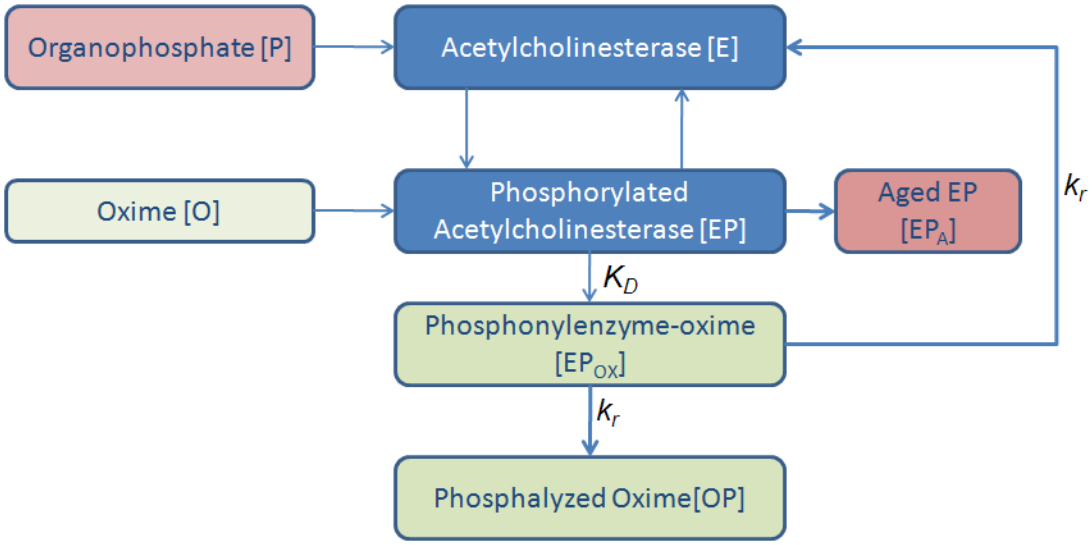

Figure 5-10. The Oxime Repair Model

The model predicts how the concentration of oxime in the blood acts on the phosphorylated acetylcholinesterase ([EP]). The result is the phosphorylated oxime ([OP]) and free acetylcholinesterase (*E*). The equations for *E* and [EP] (from Section 5.1) therefore become:

$$\frac{d}{dt}\mathrm{E} = -k_i * \mathrm{E} * [\mathrm{P}] + k_s * [\mathrm{EP}] + \frac{k_r[\mathrm{EP}][\mathrm{O}]}{K_D + [\mathrm{O}]} + R_{SYN}$$

$$\frac{d}{dt}[\mathrm{EP}] = -k_a * [\mathrm{EP}] - k_s * [\mathrm{EP}] + k_i E - \frac{k_r[\mathrm{EP}][\mathrm{O}]}{K_D + [\mathrm{O}]}$$

$$\frac{d}{dt}[\mathrm{OP}] = \frac{k_r[\mathrm{EP}][\mathrm{O}]}{K_D + [\mathrm{O}]}$$

where

k_r is the reactivation rate

K_D is the dissociation constant

The equations describing the concentration of acetylcholinesterase, *E*, and the concentration of the phosphorylated AChE/OP compound [EP] now have an additional term that describes the effect of the oxime [O]. There are two rate constants associated with this term, the reactivation rate (k_r) and the dissociation constant (K_D). The dissociation constant describes a compound's propensity for breaking down into its smaller components (in this case, AChE/OP complex and the oxime, also known as the Michaelis-type phosphyl-AChE-oxime complex). If K_D is large, the oxime tends to break apart from the complex at a faster rate, reducing the effect of the oxime. If K_D is small, the complex has a higher likelihood of remaining together long enough for the oxime to fully reactivate the AChE at a rate k_r.

The values of k_r (the reactivation constant) and K_D (the dissociation constant) are dependent on oxime and organophosphate. The values for a collection of oxime/OP pairs are shown in Table 5-8. Additionally, parameter values for OP/oxime combinations in mini-pigs are presented in Table 5-9.

Table 5-8. OP and Oxime-Dependent Parameters for Human Oxime Therapies

Agent	Unit	Obidoxime	HI-6	2-PAM	MMB-4
GA	k_r (min^{-1})	0.04[1]			0.02[2]
	K_D (μM)	97.31			24182
GB	k_r (min^{-1})	0.937[3]	0.6771	0.253	1.872
	K_D (μM)	31.63	50.11	27.63	15442
GD	k_r (min^{-1})	GD is largely resistant to oxime therapy.			
	K_D (μM)				
GF	k_r (min^{-1})	0.39[4]	1.34	.184	4.472
	K_D (μM)	9464	47.24	31594	24672
VX	k_r (min^{-1})	0.8924	0.2421	0.2154	1.562
	K_D (μM)	27.354	11.51	28.074	11962
VR	k_r (min^{-1})	0.6304	0.71[5]	0.7124	4.012
	K_D (μM)	105.94	9.155	30.654	5742

Table 5-9. Oxime and OP-Dependent Parameters for Mini-Pigs

Agent	Unit	Obidoxime	HI-6	2-PAM	MMB-4
GF	k_r (min^{-1})	0.328[6]	0.0851	0.043	1.172
	K_D (μM)	23.13	261.31	14.83	11092
VX	k_r (min^{-1})	0.071[4]	0.1374	0.0234	0.762
	K_D (μM)	945.64	712.74	896.44	16822
VR	k_r (min^{-1})	2.2994	0.0611	0.094	0.272
	K_D (μM)	183.84	448.61	274	10532

The values of k_r and K_D for obidoxime and HI-6 against a sarin exposure suggest that, for an equivalent concentration of sarin and oxime, obidoxime would have a greater efficacy than HI-6. This is because the reactivation constant for obidoxime/sarin (0.937 min^{-1}) is greater than HI-6/sarin (0.677 min^{-1}) and the dissociation constant for obidoxime/sarin (31.6μM) is smaller than HI-6/sarin (50.1 μM). Figure 5-11 shows model results for an LD_{50} of sarin administered intravenously with no treatment (blue line), and 0.7E3 μmol of obidoxime (green line) and HI-6 (red line) administered at 1 minute, 251 minutes, and 501 minutes. As the results show,

[1] (Worek F. , Eyer, Szinicz, & Thiermann, 2007)
[2] (Worek, Wille, Aurbek, & Eyer, 2010)
[3] (Worek, Reiter, Eyer, & Szinicz, 2002)
[4] (Worek, Aurbek, Wetherall, Pearce, Mann, & Thiermann, 2008)
[5] (Aurbek, Thiermann, Szinicz, & Worek, 2007)
[6] (Worek, Reiter, Eyer, & Szinicz, 2002)

obidoxime is more effective than HI-6 against sarin poisonings with estimated probabilities of mortally of 49% (no treatment), 24% (HI-6), and 22% (obidoxime).

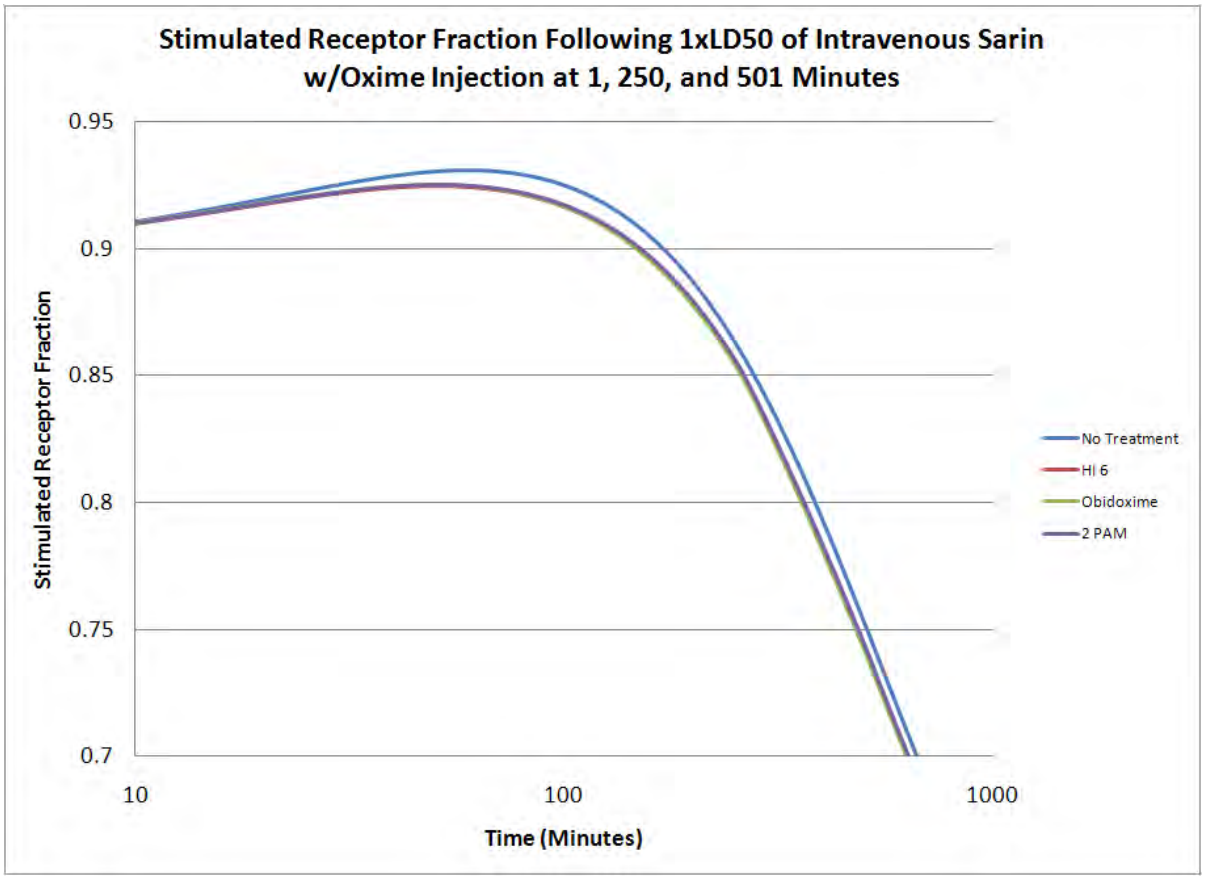

Figure 5-11. Stimulated Receptor Fractions for Three Different Treatment Regimens against an LD_{50} of Intravenous GB

A more drastic example of oxime efficacy can be seen in the case of GF combined with obidoxime and HI-6. According to the published k_r and K_D, HI-6 should have a very high efficacy for GF exposures (high reactivity, low dissociation) compared to obidoxime, which should be close to completely ineffective (low reactivity, high dissociation). Figure 5-12 shows the model results for treatment efficacies against an LD_{50} of intravenous GF. Once again, 0.7E3 µmol of oxime was administered at 1, 251, and 501 minutes. As predicted, we see a greater benefit from HI-6 treatment (red line) compared to obidoxime (blue line). The model predicts probabilities of mortality of 50% (no treatment), 45% (obidoxime), and 3.5% (HI-6).

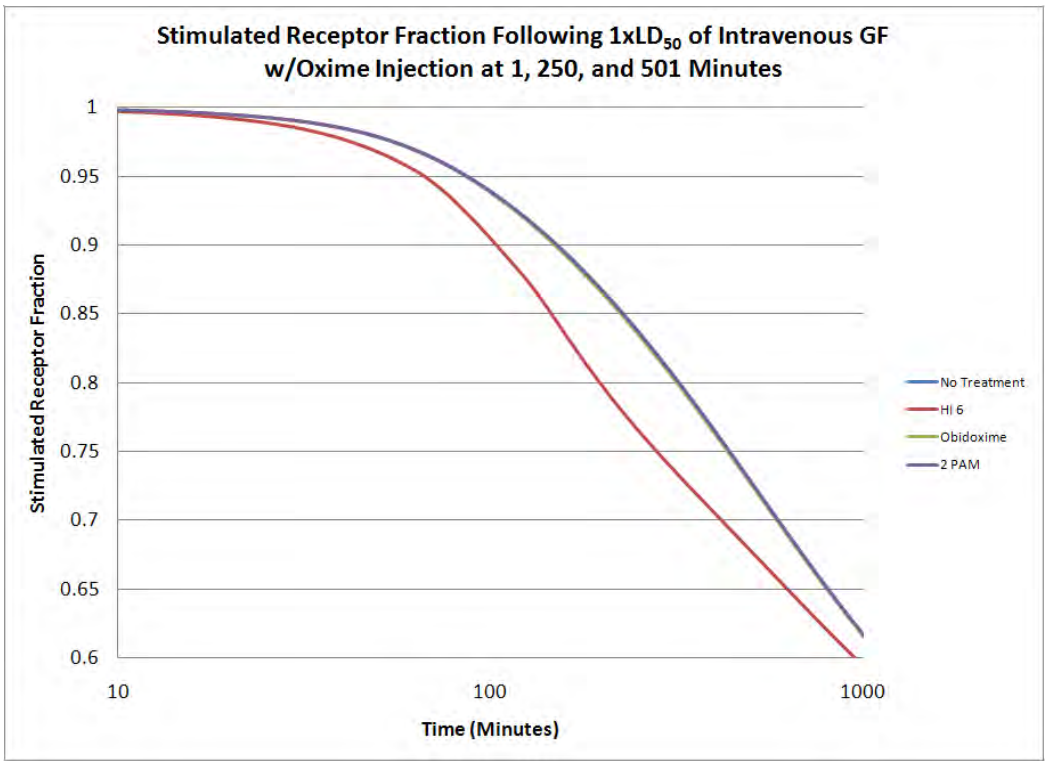

Figure 5-12. Stimulated Receptor Fractions for Three Different Treatment Regimens against an LD_{50} of Intravenous GF.

5.3 Anticholinergic Model Parameters

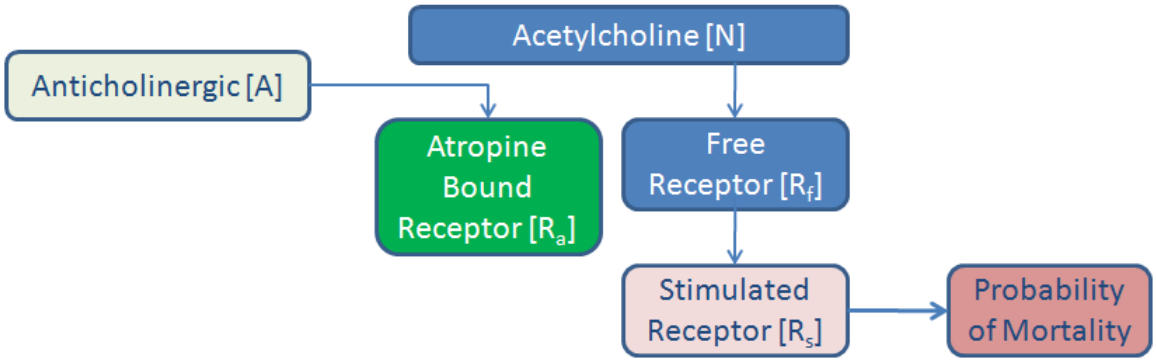

Figure 5-13. Atropine Model

Anticholinergic countermeasures (like atropine) work by competitively binding with the post-synaptic receptors, making it so acetylcholine cannot stimulate the receptors and lead to muscular tremors and respiratory failure. Since atropine and other anticholinergics reduce the number of stimulated receptors without reducing the concentration of the phosphorylated acetylcholinesterase, the introduction of atropine by itself tends to have no effect on the

likelihood of fatality for a given OP exposure. Since anticholinergics act solely on free receptors, we included them in the model with the following equation:

$$R_b = k_{block}[A] * R_f - k_{unbind} * R_b$$

$$\mathrm{R_f} = \mathrm{k_{work}E} * \mathrm{R_s} - \mathrm{k_{bind}[N]} * \mathrm{R_f} + \mathrm{k_{unbind}} * \mathrm{R_b}$$

where

R_b is the blocked receptor

k_{block} is the rate the anticholinergic binds to free receptors

k_{unbind} is the rate the anticholinergic unbinds to the free receptors

Our model assumes atropine effectiveness is independent of OP, since atropine works at the receptor level and is not hindered by the presence of OP, only by the presence of stimulated receptors. The values for these rate constants are not in the current literature. We needed to fit these parameters in order to provide recommended values. We first reviewed the literature on anticholinergics, and our findings are discussed below.

Research has shown that atropine by itself has minimal benefit in severe organophosphate poisoning cases. In one review of human OP poisoning, it was found that out of 63 patients, one subgroup treated with atropine and 2-PAM had a 100% survival rate, whereas one subgroup treated with just atropine had an 88% survival rate. Additionally, the subgroup treated with atropine and 2-PAM had more severe symptoms than the subgroup treated with just atropine (Biljana & Stojiljkovic, 2007). Since the severity of symptoms were not discussed in detail, it is difficult to correlate this information to our injury model. Also, the study was for accidental exposures to different OPs with no known dose. However, for sarin, our model predicts a concentration of 25mg/m^3 over 1 minute will produce a 12% fatality rate (88% survival rate) without oxime treatment and a 3.5% survival rate if the person is treated with 2-PAM at 1 minute. Whereas these exposures and treatments do not directly correlate to this study, the results at least show some consistency with survival rates for real exposures.

One study of the Tokyo sarin attack (Yanagisawa, Morita, & Nakajima, 2006) mentions that some severely injured individuals (loss of consciousness, seizures, etc.) recovered after being treated with a combination of atropine and benzodiazepines. Oxime treatment is not mentioned for these patients but neither is specific dosing or severity of symptoms.

A study conducted on OP poisonings in India looked at two different groups of patients suffering from accidental OP poisoning (Chugh, Aggarwal, Dabla, & Chhabra, 2005). One group of 15 people was treated solely with atropine at 2mg intervals every 5-10 minutes until signs of atropinisation appeared (dilated pupils and elevated heart rate). The second group of 15 patients were given atropine intermittently and 2-PAM intravenously at 1g every 6 hours. In both groups, the cholinesterase activity levels were measured at daily intervals over a 4-day period. The cholinesterase activity level appeared to have risen in a similar manner for both groups (Figure 5-14). Also, one individual that received a combination of atropine and 2-PAM died, compared to no deaths in the group receiving just atropine. However, since we do not know the severity of illness for the different individuals (with the exception of the fact that the atropine + 2-PAM individuals seemed to have slightly higher cholinesterase activity levels at the onset and, one

could conclude, slightly less severe poisonings on average), it is difficult to correlate treatment regimens to actual effectiveness.

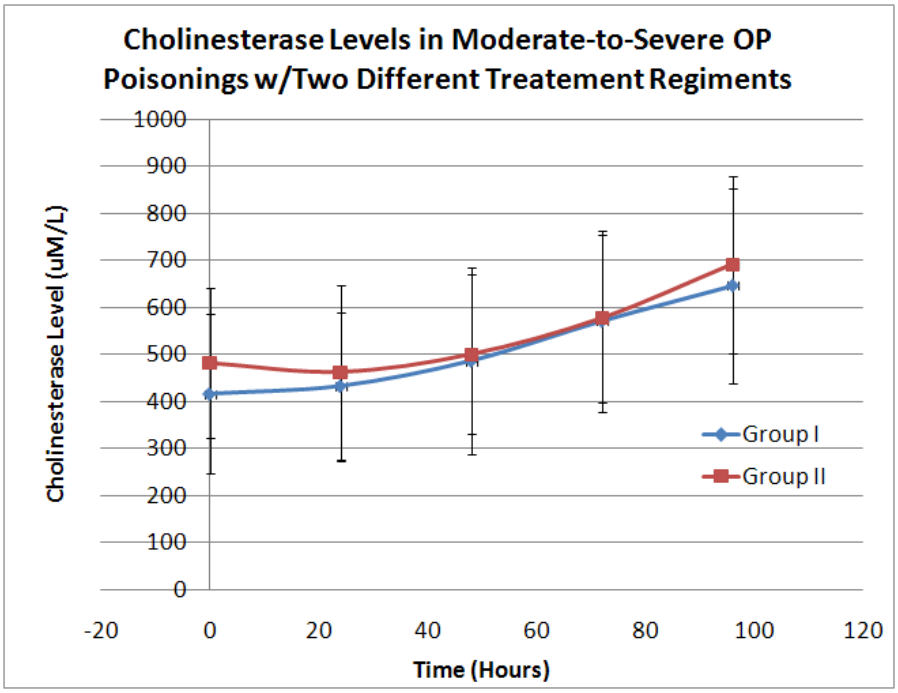

Figure 5-14. Cholinesterase Levels of 15 Individuals Receiving just Atropine (Group I) and 15 Individuals Receiving Atropine and 2-PAM (Group II) (Chugh, Aggarwal, Dabla, & Chhabra, 2005)

In a guinea pig experiment (Skovira, O'Donnell, Koplovitz, Kan, McDonough, & Shih, 2010) it was shown that atropine alone offers no benefit against an LD_{50} dose of GB, GF, or VX. However, it was shown that atropine + 2-PAM compared to 2-PAM in the absence of atropine increased the LD_{50} ratio GB. Atropine may not cause a significant benefit on its own, it may increase the efficacy of oximes, whereas our model looks at the effect atropine may have on delaying the binding of free receptors. Some researchers suggest atropine helps oximes cross the blood-brain barrier (Wagner, et al., 2010). Since we are not modeling dispersion of the agent throughout the body with this model, we needed to try and capture the overall beneficial effects of atropine by looking at how it affects the free/stimulated receptor ratio. In the experiment, an LD_{50} dose of GB was administered intravenously, followed 1 minute later by either .5mg/kg of atropine, 25mg/kg of 2-PAM, or .5.g/kg of atropine + 25mg/kg of 2-PAM. In the experiment, atropine alone had no effect of the LD_{50}, 2-PAM doubled the LD_{50}, and atropine + 2-PAM provided a protection ratio of 3.3.

Since we do not have a toxicokinetic model of atropine distribution in a guinea pig, we first modeled the effect of a $2xLD_{50}$ dose of intravenous sarin in a human, followed 1 minute later by a 25mg/kg dose of atropine (assuming a 70kg human, 1750 mg of 2-PAM or 5 mmol of 2-PAM). The model predicted a 45% probability of mortality (compared to 49% for $1xLD_{50}$ of sarin with no treatment). We assumed that in the human model, the results were closely following that of a guinea pig. We then modeled the probability of mortality for the same dose of 2-PAM against

3.3xLD_{50} of intravenous GB, given at 1 minute post-exposure and calculated a probability of fatality of 97%. Figure 5-15 shows the free receptor fraction as a function of time for the above scenario. As shown, at 1 minute the free receptor fraction is 0.2, the point at which an individual starts to accumulate a probability of mortality. It is apparent that the atropine must act fast in order to decrease the probability of mortality to 50%. By 3 minutes the free receptor fraction is close to 0, resulting in the high probability of mortality.

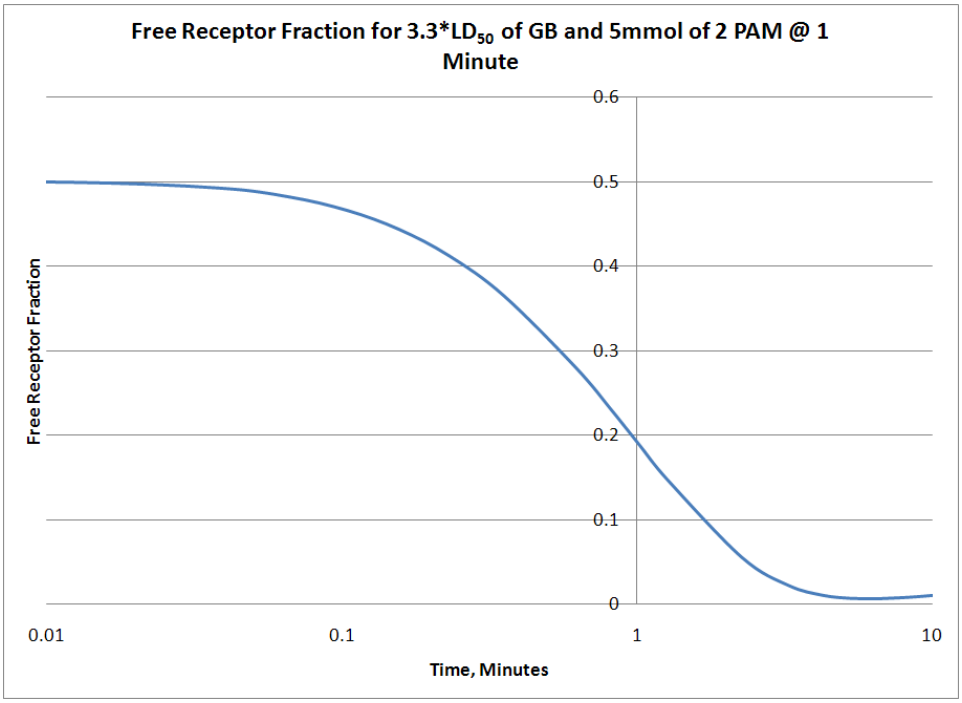

Figure 5-15. Free Receptor Fraction for 3.3xLD_{50} and 2-PAM Treatment without Atropine

Atropine pharmacokinetics were studied in swine (Hörnchen, Schüttler, Stoeckel, Ensing, de Zeeuw, & Eichelkraut, 1989). Atropine was shown to rapidly disseminate in the blood, with endobronchial administration achieving a peak plasma concentration after 2 minutes and intravenous injections achieving a peak plasma concentration after 1 minute. Because of this, we are assuming a near instantaneous effect of atropine concentration in the blood. Therefore, the equation for [A] can be equal to:

$$\frac{\mathrm{d}}{\mathrm{dt}}[\mathrm{A}] = \mathrm{pulse}(\mathrm{A}_0, \mathrm{A}_{\mathrm{time}}) - \mathrm{k}_{\mathrm{bind}} * [\mathrm{A}] * \mathrm{R}_{\mathrm{f}}$$

where

A_0 is the initial dose of atropine in μmol

A_{time} is the time of atropine administration

The pulse function has a value of A_0 at time A_{time}. When integrated, it results in a step function of height A_0.

In order to fit k_{bind}, we used the administered dose in a guinea pig (0.5 mg/kg) and scaled it to a 70kg man (35 mg or 1.21E-1μmol) and fit k_{bind} in Berkley Madonna to get predicted values for k_{bind} (0.263) and k_{unbind} (0.031). The resulting probability of mortality against 3.3xLD_{50} was 50%.

5.4 Anticonvulsant Model Parameters

Anticonvulsants such as diazepam greatly reduce the occurrence and severity of seizures, but have not been shown to have any effect on the Probability of Mortality. Diazepam works by depressing the central nervous system, thus slowing the release of ACh. The effect that anticonvulsants have in our model is to decrease the concentration of ACh [N] and slow down the rate at which it binds to free receptors. Therefore, the equation for ACh becomes:

$$[\mathrm{N}] = \mathrm{K_{release}} - \mathrm{k_d}[\mathrm{D}]\mathrm{K_{release}}$$

[*D*] is the concentration of diazepam and k_d is the rate at which diazepam depresses the CNS and slows the release of [N]. This equation for [N] was chosen so that the diazepam will slow the release of ACh as long as it's in the body. In order to model the diazepam in the body, we used an equation similar to atropine, but with a clearance term as a sink instead of the binding rate. This gives us:

$$\frac{\mathrm{d}}{\mathrm{dt}}[\mathrm{D}] = \mathrm{pulse}(\mathrm{D_0}, \mathrm{D_{time}}) - \mathrm{D_{clear}}$$

where

D_0 is the initial dose of diazepam in μmol

D_{time} is the time of diazepam administration

D_{clear} is the clearance rate of atropine in μmol/min^{-1}

One study used two dosing regimens in guinea pigs in order to measure the effectiveness of three anticonvulsants: diazepam, midazolam, and scopolamine. Both sets of guinea pigs were given a subcutaneous 2xLD_{50} OP exposure. One group was given 2mg/kg of atropine and 25mg/kg of 2-PAM 1 minute after the exposure and the anticonvulsant was given 5 minutes after onset of seizures. The second group was given 0.1 mg/kg of atropine and 25mg/kg of 2-PAM 1 minute after the exposure and the anticonvulsant at seizure onset. The study aimed to measure probability of lethality, onset of signs and symptoms, time to death, and seizure occurrence for the two groups. We decided that this was a good dataset for fitting and testing the diazepam model.

Interestingly, average onset of seizure had a significant decrease for GB, GF, and VX-exposed animals for the lower atropine regimen. We can simulate the difference between intravenous exposures of sarin in humans with equivalent dosings in order to see if there is a noticeable difference in stimulated receptor fractions between the different dosing regimens. The result of this simulation is shown in Figure 5-16. As the model predicts, the higher atropine dose results in a significant decrease in the stimulated receptor fraction as well as a significant decrease in the probability of mortality (35% compared to ~100% for the other three doses). Since we are not yet correlating signs and symptoms to stimulated receptor fraction we can at

least look at this qualitative simulation and say that the addition of atropine is giving the oxime enough time to reactivate the acetylcholinesterase and begin to cleave to the stimulated receptors that would have otherwise been occupied if the high dose of atropine wasn't administered. This could very well lead to a decrease in onset time.

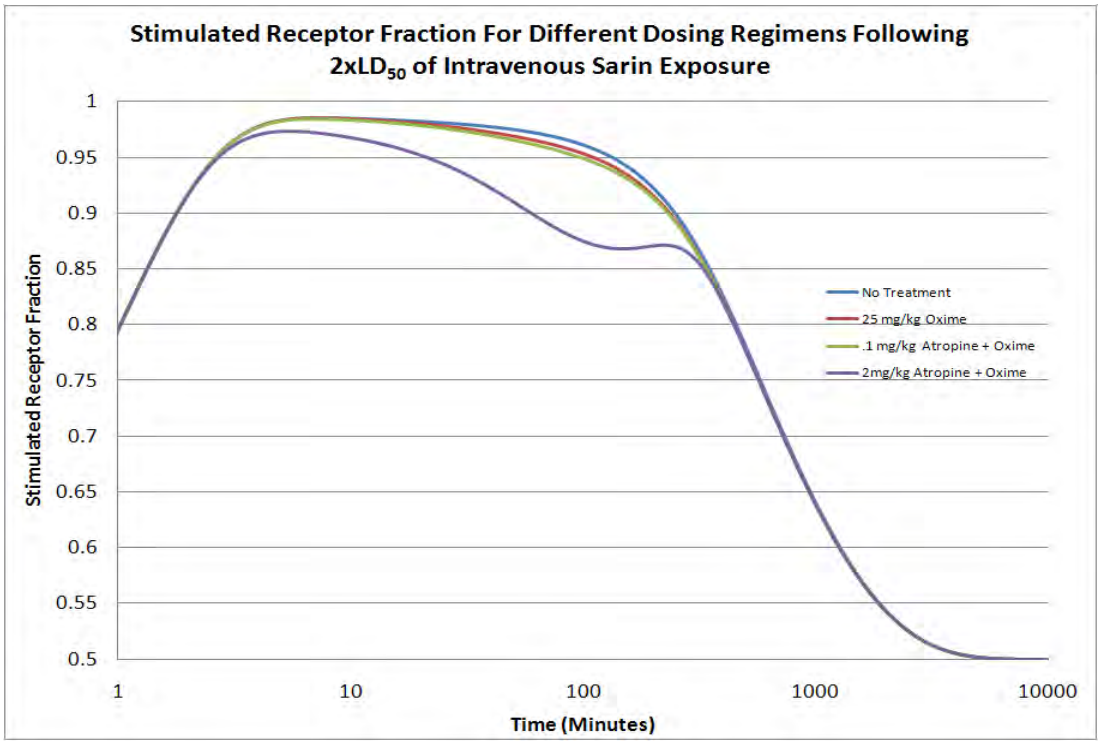

Figure 5-16. Stimulated Receptor Fraction for Varying Dosing Regimens Following 2xLD$_{50}$ Exposure of Intravenous Sarin

Since probability of mortality is the primary output of our model, however, we need to look at the probability of mortality for the two dosing regimens. The low dose of atropine, which was coupled with oxime and diazepam at symptom onset resulted in a probability of mortality of 25% (compared to 98% in our model without diazepam). The high dose of atropine, which was coupled with oxime and diazepam five minutes after the onset of symptoms, resulted in a probability of mortality of 0% (compared to 35% in our model). The beneficial effects of diazepam when combined with atropine and oxime are apparent, based on this comparison.

In order to account for diazepam in our equations, we first needed to account for administration time. Since the low dose of atropine/oxime/diazepam combination resulted in an average onset time of 6.08 minutes and since the study administered the diazepam at seizure onset, for that model, we assumed diazepam was administered at exactly 6.08 minutes. For the higher dose of atropine regimen, where the average onset of seizures was at 8.45 minutes, we assumed that the diazepam was administered at 13.45 minutes (5 minutes after symptom onset, as in the study).

Without a toxicokinetic study of diazepam clearance in humans, we set the value of D_{clear} to 0.005 μmol/min^{-1} to keep the biological clearance rate similar to the nerve agents. This just left

the value of k_d for which, using Berkley Madonna and the low atropine dosing regimen (2.4E-2μmol atropine, 10μmol 2-PAM, 2.5μmol of diazepam), we calculated a value of 0.331. This resulted in a probability of mortality of 24.9%, compared to 25% in the study. We then reran the simulation with the higher atropine dosing regimen (4.8E-1 μmol) and a later diazepam administration time (13.45 minutes) and calculated a probability of mortality of 1%, compared to 0% in the study. Interestingly, when simulating diazepam administration at symptom onset (6 minutes) with the higher atropine dose, we calculated a probability of mortality of 0.87%, a slightly higher increase in the probability of mortality. Since we did not find a study that compares the effect of diazepam administration time on the efficacy of treatment regimens, we cannot verify whether or not this simulates reality. However, in both cases, most of the acetylcholinesterase that would have been inhibited has already been inhibited by the OP at the time of diazepam administration, resulting in a greater number of stimulated receptors. Slowing the release of ACh at an earlier time, when most of the receptors are bound, wouldn't have that great of an effect. Intuitively, it would make sense that slowing the release of the ACh at any time when there are free receptors available as well as AChE to cleave the stimulated receptors, would lead to a greater efficacy of the drug. Table 5-10 shows the calculated probability of mortalities for varying administration times. The probability of mortality decreases between an administration time of 6.01 minutes and 60 minutes. At 180 minutes, we see that the probability of mortality begins to rise again. At 500 minutes, there is no benefit from diazepam administration. For the scenario where diazepam was administered at 500 minutes, the stimulated receptor fraction had already dropped below 0.8, simply due to oxime function and biological repair. Therefore, the diazepam would have no effect on probability of mortality. It could (and probably would) have an effect on severity of symptoms, however.

Table 5-10. Probability of Mortality for Varying Administration Times of Diazepam against 2xLD_{50} of GB

	Administration Time (Minutes)								
	0	**6.01**	**13.45**	**20**	**30**	**60**	**180**	**240**	**500**
Probability of Mortality	0.9%	1.1%	1.03%	1.02%	1%	0.9%	1.4%	4.1%	35.6%

5.5 Bioscavenger Model Parameters

Bioscavengers remove organophosphates from the body while in the blood stream and are meant to be administered as prophylaxis. Bioscavengers have been shown to have a significant protective ability in animals; there have been no human trials of bioscavenger efficacy. Since bioscavengers work to sequester the OP that is in the blood, they can be included in our model by decreasing the concentration of OP as it enters the body.

In one study (Valiyaveettil, et al., 2011), human paraoxonase (PON1) administered 30 minutes prior to an OP exposure of 1.2xLD_{50} showed an increase in survival of guinea pigs from 14% up to 67%, when challenged with sarin and 20% to 75%, when challenged with soman.

In another study (Doctor & Saxena, 2005), the efficacy of human serum BuChE (HuBuChE) was studied in mice, guinea pigs, and moneys. Ten guinea pigs were pretreated with HuBChE at a level designed to protect up to 8xLD_{50} of GD or VX, assuming a 1:1 ratio of HuBChE molarity to OP molarity in the blood. At 19 hours post HuBChE administration, the animals were

challenged with up to 5.5xLD_{50} of GD and 5xLD_{50} of VX. In both cases, all animals (10 from each group) survived and no animals exhibited any signs or symptoms of OP poisoning. A similar experiment was conducted on monkeys, except with 75 mg of HuBChE followed by sequential doses of 1.5, 2.0, and 2.0xLD_{50} of soman. Of the six monkeys, one died, one exhibited severe effects, and four showed no signs of OP poisoning. The four that showed no signs of OP poisoning were studied for any long-term health effects and none have been reported after several months of observation.

It is apparent that HuBChE allows for significant protection in guinea pigs and monkeys, and has been chosen as the candidate bioscavenger for human prophylaxis. It is also apparent that the rate at which the bioscavenger sequesters the OP is almost instantaneous, so we do not need to account for a theoretical scavenging rate. The Doctor & Saxena study mentioned above, as well as a review of HuBuChE experiments in animals (Lenz, Yeung, Smith, & Sweeney, 2007), both quoted a 1:1 ratio for neutralized OP molecule to bioscavenger. This means that a given molarity of bioscavenger will directly decrease a given molarity of OP; therefore, bioscavengers alter [P] via the following equation:

$$\frac{d}{dt}[P] = -[B]$$

where

$[B]$ is the concentration of the bioscavenger in the blood in μmol.

The bioscavenger is administered as prophylaxis, so there is no need to model its introduction into the body. Studies have shown that the OP needs to be scavenged within one blood circulation time period (7 minutes for humans) in order to be effective (Raveh, Grunwald, Marcus, Papier, Cohen, & Ashani, 1993). This means that post-exposure application would likely do nothing to neutralize the OP (except maybe in protracted exposures) and also verifies, again, that the rate of scavenging would be very fast. We assume a constant level of bioscavenger at the time of exposure. The bioscavenger concentration then decreases as it sequesters the OP from the blood, as given by the following equation:

$$\frac{\mathrm{d}}{\mathrm{dt}}[\mathrm{B}] = -[\mathrm{P}]$$

where [B] is limited to being greater than or equal to one. This will allow for protection from multiple exposures to OP as long as there is still bioscavenger present in the blood.

This page is intentionally left blank.

Section 6.

Discussion

6.1 Model Comparison to Human Data

There is limited human data that correlates AChE activity to OP poisoning *in vivo*. One paper was found that presented the AChE activity of 20 individuals in the acute phase, admitted into the hospital following the Tokyo sarin attack. The lowest value AChE activity reported was 7% and the highest was 96%. Persisting health effects one year post-event were studied in these individuals and no one with an AChE activity above 33% was exhibiting any signs or symptoms that could be considered a consequence of the sarin exposure (with one exception). Conversely, everyone with an AChE activity below 33% was exhibiting chronic problems that could be associated with sarin exposure. Figure 6-1 shows that the model predicts an ECt_{10} for Severe Effects to correlate to a minimum AChE % of approximately 30%. Anything less than that value falls well within the ICt for severe effects and the LCt range. Figure 6-1 reproduces Figure 4-4 with the measured human AChE % for individuals admitted to the hospital. The purple diamonds are individuals who had severe enough effects so as to still be experiencing effects one year later and the blue squares are individuals who had severe enough effects to be admitted to the hospital but who did not experience any additional symptoms one year later. There is an obvious correlation between severity of effect, AChE %, and chronic health effects as shown. We believe this further validates the human model, even though the actual dose or sign/symptoms experienced by the users is unknown.

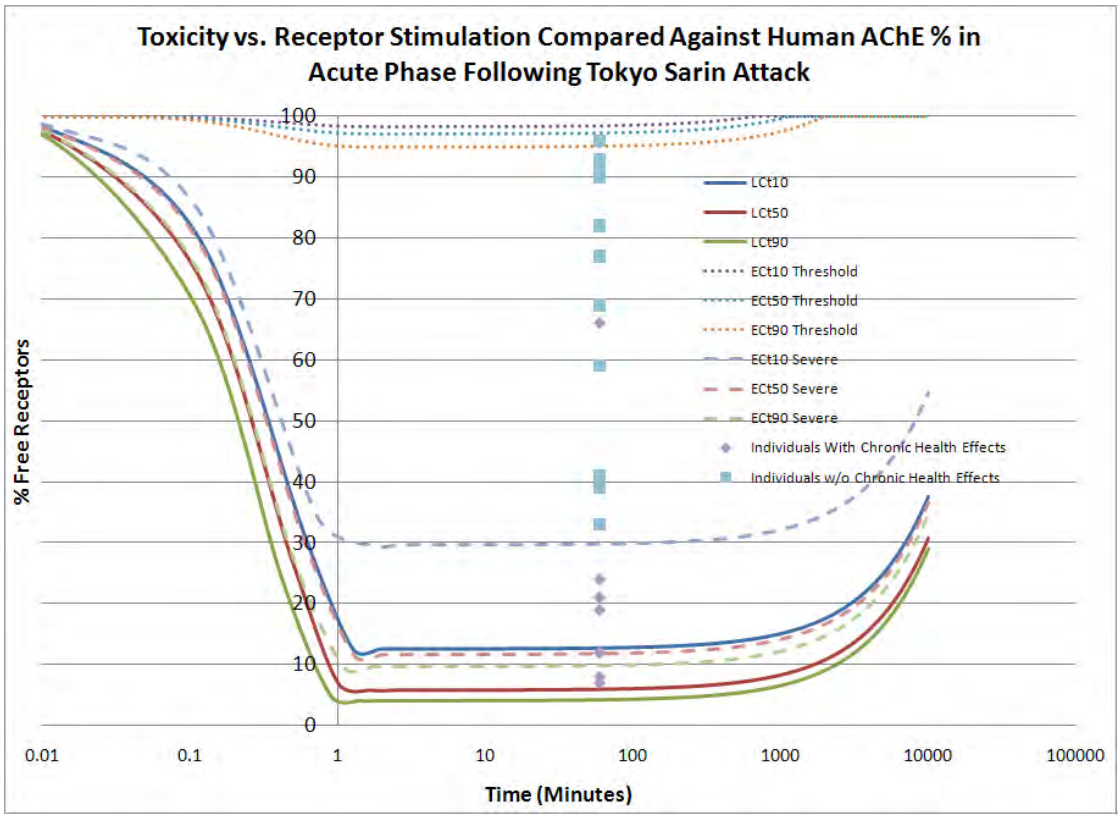

Figure 6-1. Sarin Model Output Compared to Individual AChE Activity in Acute Phase Following Tokyo Sarin Attack

6.2 Model Comparison to Animal Data

Due to the lack of *in vivo* data in controlled human experiments, we needed to compare model output using our animal parameters to recreate experiments performed *in vivo*.

6.2.1. Verifying AChE Activity

One measure of model performance that helps us validate the biological components of our model is to compare measured AChE activities in animal experiments against model predictions for activity. We found two studies that fit within the confines of our model. Both were looking at the therapeutic effects of 2-PAM against sarin, VX, and VR to compare the efficacies of novel oximes. In both studies, the sarin was injected into a guinea pig intravenously. Since our model allows us to study the combination of intravenous exposure, sarin, 2-PAM, and guinea pigs, this was an ideal series of experiments for us to focus on and attempt to emulate.

Figure 6-2 shows the results of the guinea pig model compared against experimental data from an *in vivo* study of sarin exposure done by Skovira, 2010. In the experiment, researchers exposed guinea pigs to sarin, VX, VR intravenously and introduced oximes (or, in the case of the control, introduced no oximes) at five minutes post-exposure. The animals were sacrificed at 60 minutes and the AChE activity was evidenced in their diaphragm, heart, skeletal muscle, RBC, and whole blood. Since our model does not currently account for the distribution of the OP to different organs, our best point for comparison is to the whole blood results. As seen in the figure

below, the model prediction intersects the measured AChE % for whole blood at 60 minutes. Similar comparisons in this section will continue that trend.

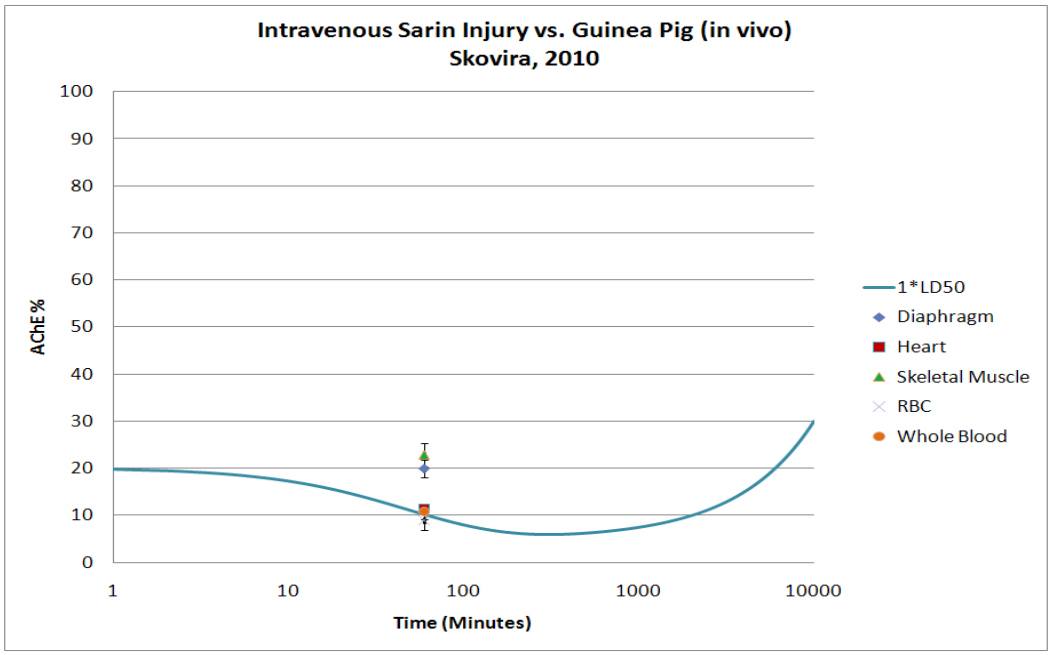

Figure 6-2. Guinea Pig Injury Model for Sarin Exposure Compared against Data from Skovira, 2010

A similar experiment conducted by Shih, 2010, also treated the guinea pigs at 5 minutes and measured the AChE activity at 60 minutes. As once again seen in Figure 6-3, the model predictions closely follow the estimated value for whole blood AChE activity.

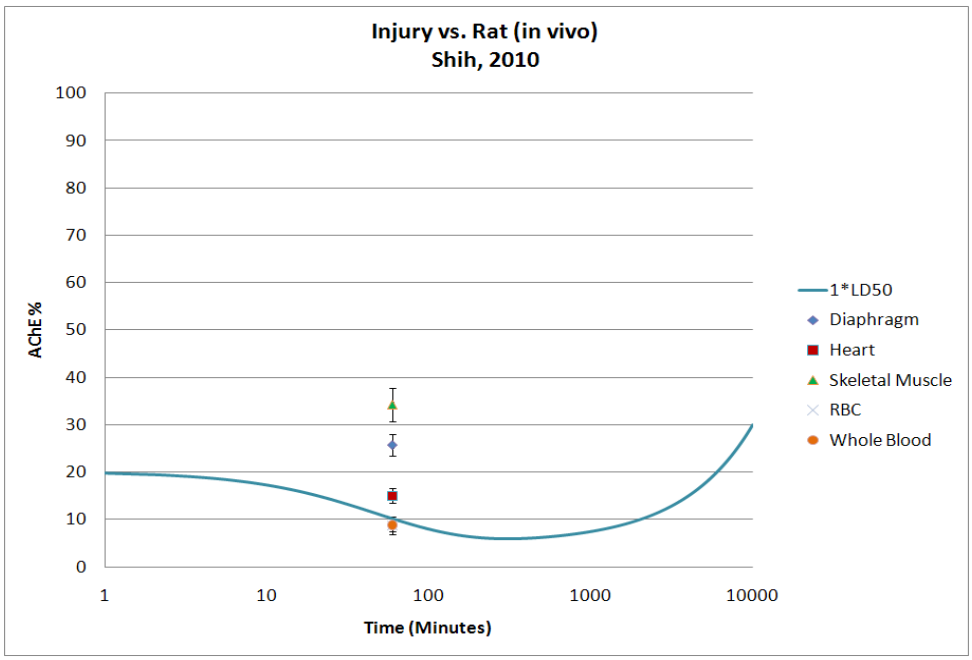

Figure 6-3. Guinea Pig Injury Model for Sarin Exposure Compared against Data from Shih, 2010

Figure 6-4 shows the results of the sarin/intravenous/2-PAM model compared against data from Skovira, 2010.

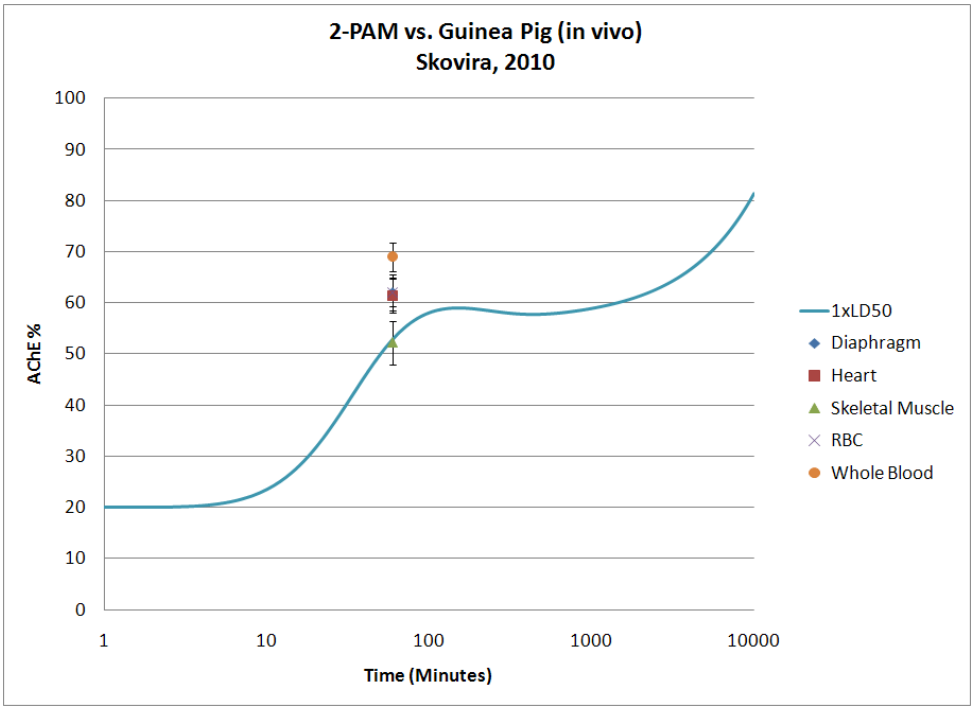

Figure 6-4. Guinea Pig 2-PAM Model for Sarin Exposure Compared against Data from Skovira, 2010

As shown in the above graph, the model prediction is now more in line with the measured skeletal muscle value than whole blood value. This shows that the model is potentially underestimating the benefit from 2-PAM treatment, but is still in line with overall reactivation in the body. In fact, Figure 6-5shows that the model prediction for 2-PAM treatment is much closer to the whole blood AChE activity in Shih's study and intersects the RBC value. This shows that there is significant variability between studies and that our model's prediction is within the range of AChE activity within different compartments.

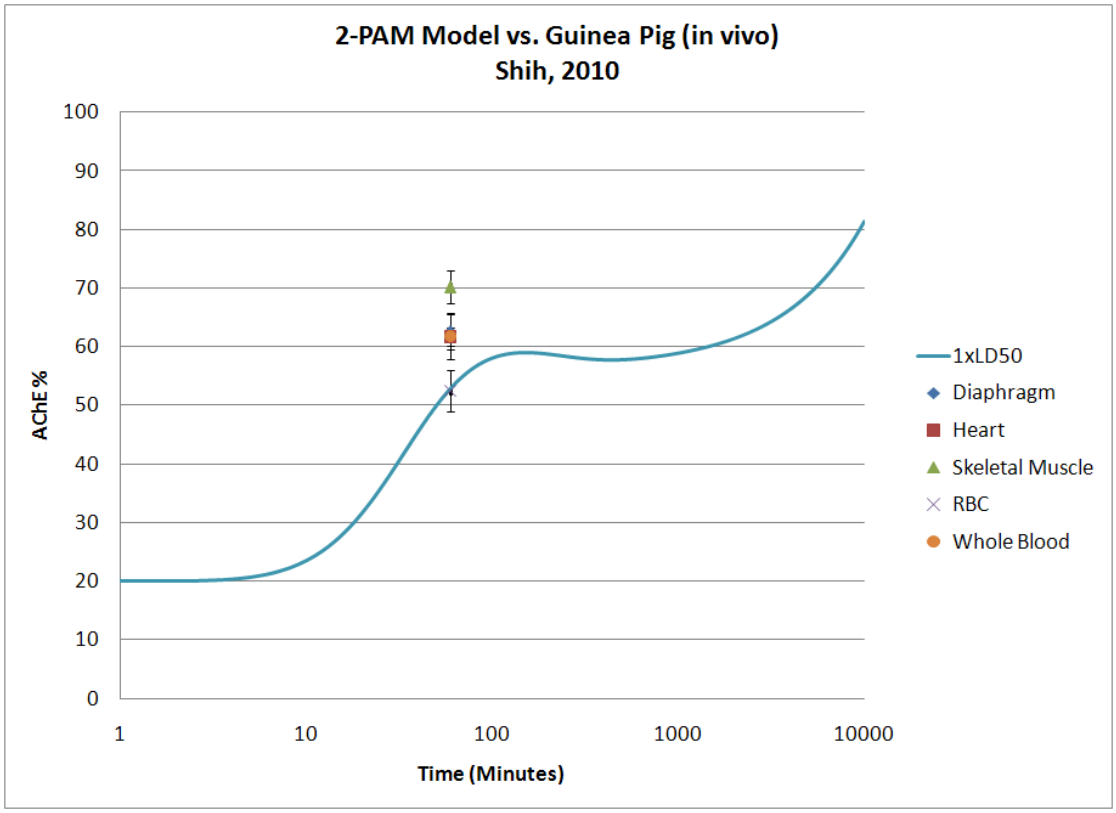

Figure 6-5. Guinea Pig 2-PAM Model for Sarin Exposure Compared against Data from Shih, 2010

6.2.2. Probability of Mortality Comparisons

Most published research aims to determine the protection factor afforded by various combinations of atropine, oximes, and diazepam. These studies provided us with the greatest level of confidence in our model, as probability of mortality is our main output.

One study that we were able to emulate looked at the effect of atropine, 2-PAM, and diazepam in guinea pigs that were intravenously exposed to $2xLD_{50}$ of GB (Koplovitz, Schulz, Raile, M., & Lee, 2007). In this study, the guinea pigs were given 25mg/kg of 2-PAM and three different atropine doses (.3mg/kg, 3mg/kg, and 16mg/kg) at 1 minute post-exposure. When we simulated the experiment with our model, we first looked at the probability of mortality, AChE activity, and stimulated receptor fraction for a guinea pig with no treatment, to ensure we received 100% fatality. We also examined a guinea pig administered with just atropine, to ensure

that the probability of fatality remained high; a guinea pig administered with just 2-PAM, to ensure that there was some beneficial effect from 2-PAM; and finally, a guinea pig administered with the atropine regimens, to ensure that there was an amplified effect when the two treatments were used together. Figure 6-6 shows the results for the stimulated receptor fraction for each of these combinations.

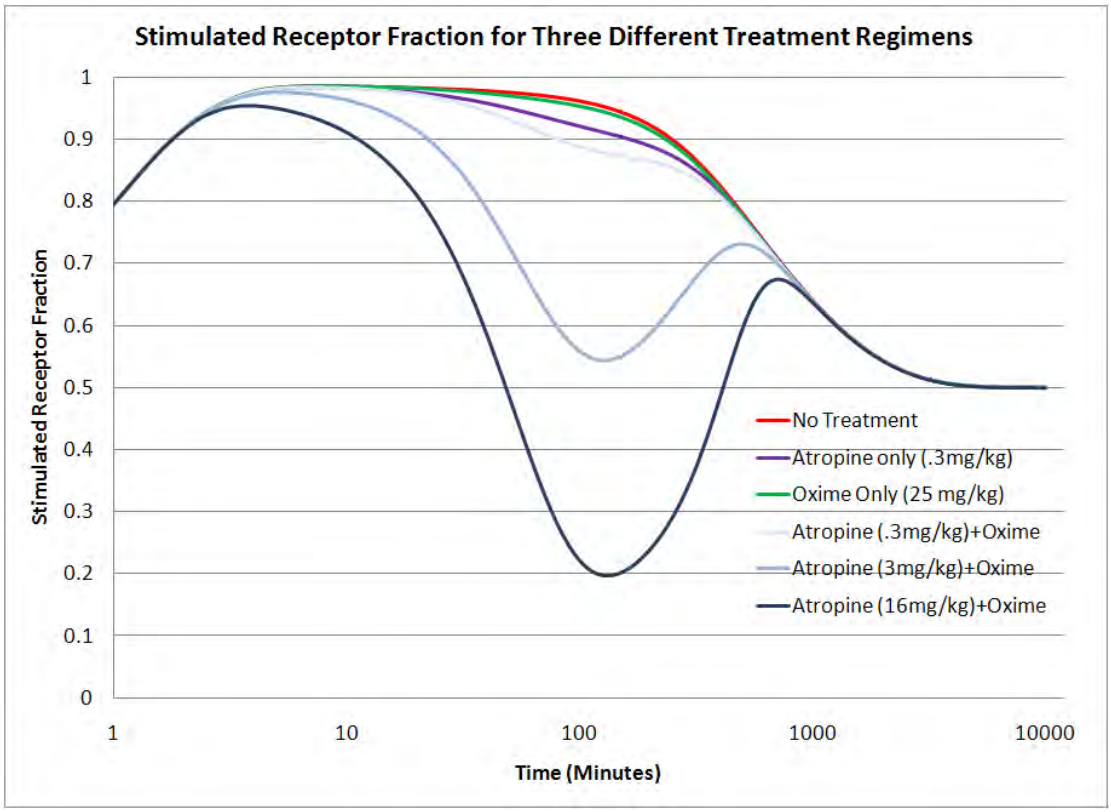

Figure 6-6. Stimulated Receptor Fraction for Different Combinations of Atropine and Oxime

The model predicted a 99% probability of mortality if the guinea pig is untreated, a 94% probability of mortality if the guinea pig is treated with just atropine, and a 98% probability of mortality if the guinea pig was treated with just 2-PAM. So, taken alone, none of these treatments led to an increased benefit in guinea pig survival. However, when the low dose of atropine was combined with 2-PAM, the probability of mortality was predicted to be 26%, compared to 30% in the literature. When the middle dose of atropine was combined with oxime, the probability of mortality was close to zero (0.05%), compared to 5% in the experiment. When the high dose of atropine was combined with oxime, the probability of mortality was 0.03%, compared to 0% in the experiment.

Whereas the comparison is very close, we still believe we are overestimating the effect of atropine, especially evidenced by the 5% decrease in probability of mortality alone, which was greater than the decrease of oxime alone. One possibility is that we are not yet accounting for the negative impact of atropine, since a blocked receptor will stop overstimulation, but receptors that

are in need of stimulation will not be able to do their job, either. We recognize this as a limitation of the model, and further research would be required at some point, to account for this effect.

The study also looked at the effect of 1mg/kg of diazepam injected one minute post-exposure for each of the three atropine+oxime combinations. For sarin, all of the dosing regimens resulted in all animals surviving. In our model, we predicted a decrease in the probability of mortality (21% for the low dose of atropine, and 0% for the middle and high dose), but for the combination of .3mg/kg of atropine, 25mg/kg of 2-PAM, and 1mg/kg of diazepam, our answer of 21% probability of mortality (down from 26% without diazepam) was still higher than the measured mortality rate. However, our data was calibrated to a study where the oxime dose was the same, the atropine dose was one-third less, and the diazepam dose was 10 times higher. With that dosing regimen, the experimenter saw a 25% probability of mortality. There appears to be disagreement between the two studies, and further investigation may be needed, to know to which dataset we should calibrate. For now, we kept our initial fit of diazepam parameters, but acknowledge that it could be overestimating the effect of diazepam.

6.3 Model Comparison to Allied Medical Publication-8

Allied Medical Publication-8 (AMedP-8) is a casualty estimation model for human battlefield exposures to chemical, biological, nuclear, and radiological insults and injuries. AMedP-8(A) and AMedP-8(B) used the CBRN human effects models to calculate unit performance and battle effectiveness for a wide combination of agents, weapons, and unit types. AMedP-8(C) departed from the methodology developed in previous versions by first, refining the human injury models by updating them with new data, then by exposing the models and the methodology behind using them, so the users can calculate casualties for exposures relevant to their mission.

6.3.1. Inhaled Sarin Comparison

As a result of this new approach, AMedP-8(C) published the time-dependent sign/symptom severity plots used in AMedP-8(A) and (B)'s underlying results. For sarin, AMedP-8(C) published the time-dependent sign/symptom severity values for six different dose bands that are designed to correspond to increasing severity of injury:

- 0.2 mg-min/m^3 – 1.0 mg-min/m^3 – Threshold effects; minor respiratory and ocular issues.
- 1 mg-min/m^3 – 6.5 mg-min/m^3 – Moderate and prolonged ocular effects, prolonged and minor respiratory effects
- 6.5 mg-min/m^3 – 12 mg-min/m^3 – Moderate ocular and neurological effects, minor respiratory effects.
- 12 mg-min/m^3 – 25 mg-min/m^3 – Severe and prolonged ocular effects, short-term severe respiratory and muscular effects. Minor-to-moderate upper and lower GI effects.
- 25 mg-min/m^3 – 30 mg-min/m^3 – Severe ocular, muscular, respiratory, neurological, and upper GI effects. Moderate lower GI effects.
- > 30 mg-min/m^3 – Fatality-causing muscular, respiratory, and neurological effects, within minutes, post-exposure.

In order to validate our models against AMedP-8, we compared the output for stimulated receptor fraction from the sarin inhalation model (1 minute exposure) against AMedP-8(C)'s sarin inhalation sign/symptom severity profiles. The resulting graphs are shown in Figure 6-7, Figure 6-8, Figure 6-9, Figure 6-10, Figure 6-11, and Figure 6-12. Discussion of results follows the figures.

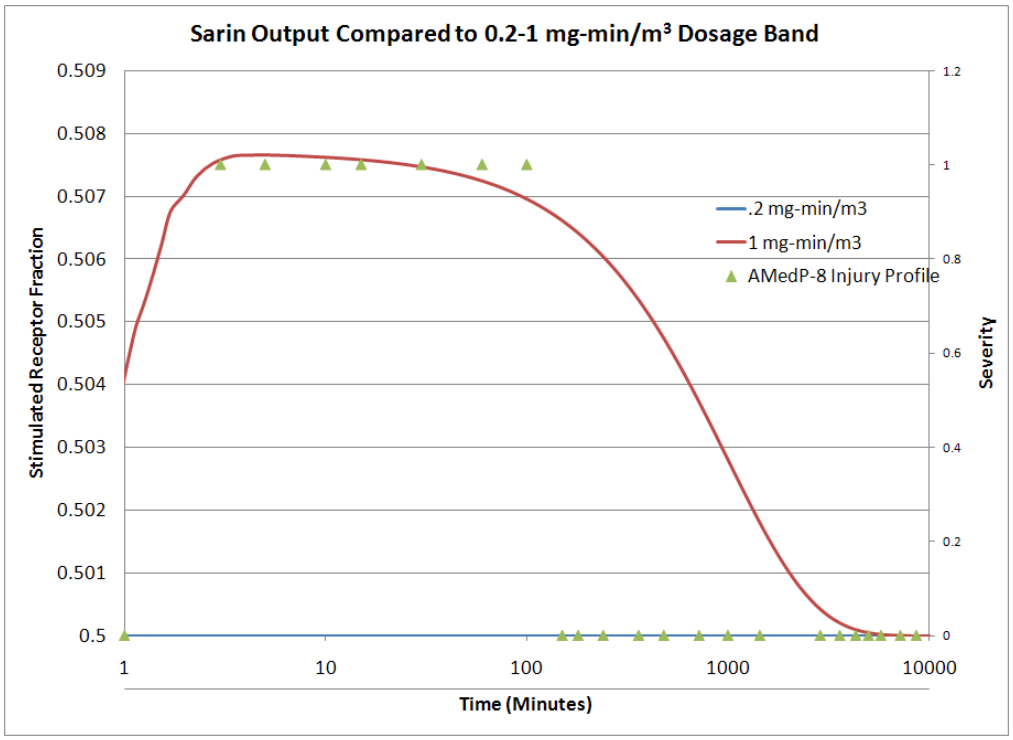

Figure 6-7. Model Results Compared to AMedP-8(C) 0.2 - 1 mg-min/m^3 Dosage Band for Inhaled Sarin

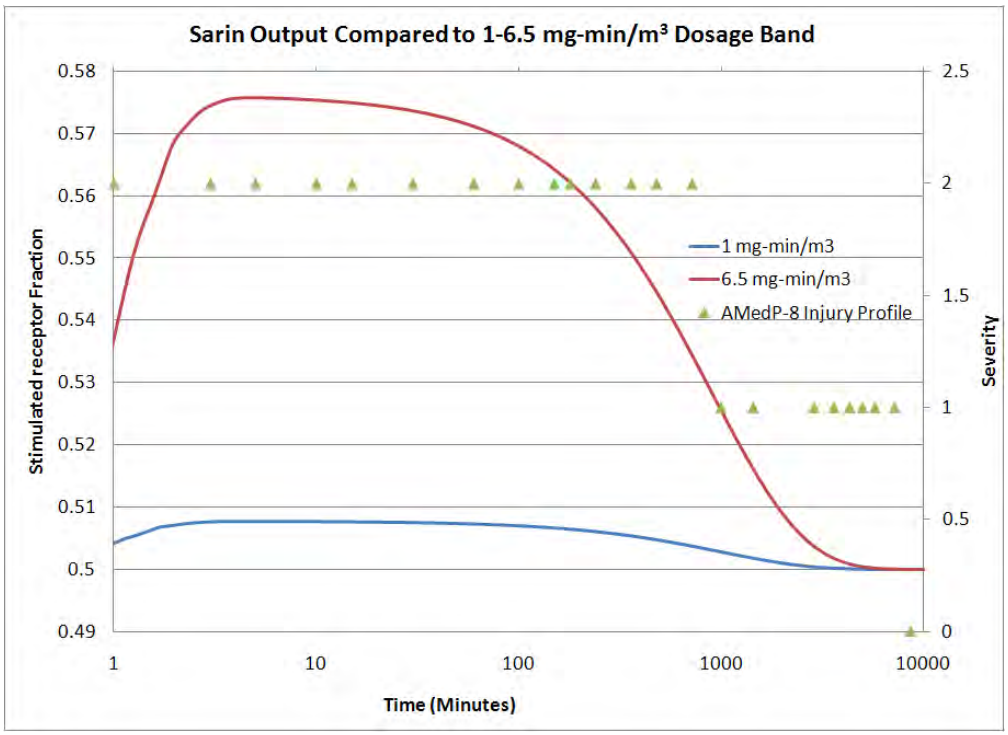

Figure 6-8. Model Results Compared to AMedP-8(C) 1 – 6.5 mg-min/m^3 Dosage Band for Inhaled Sarin

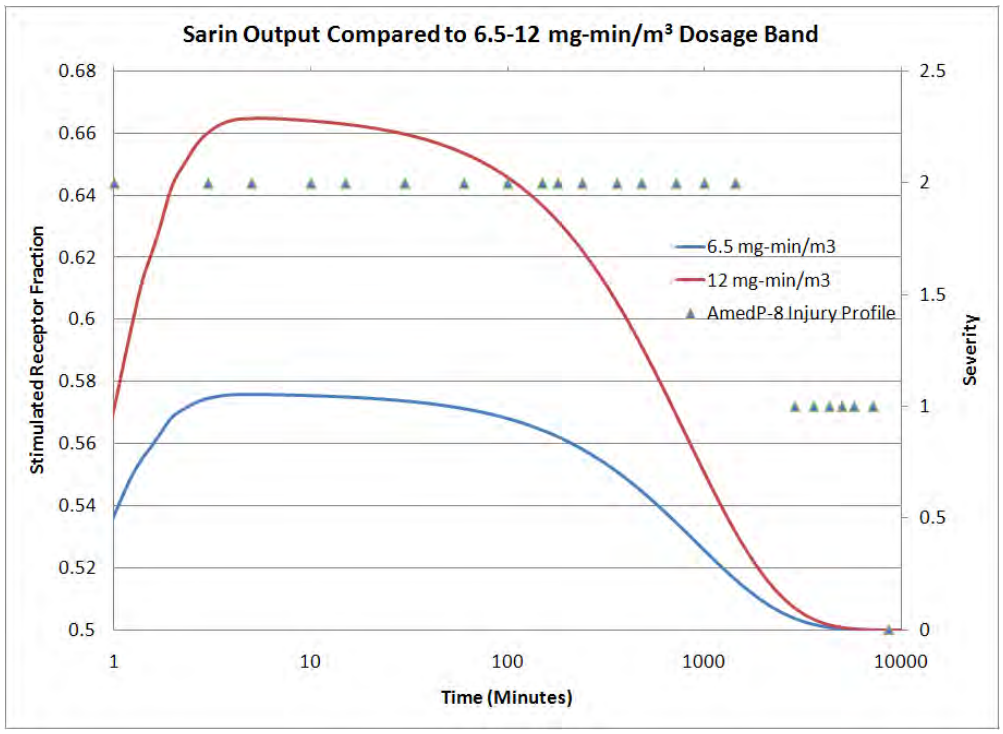

Figure 6-9. Model Results Compared to AMedP-8(C) 6.5 – 12 mg-min/m^3 Dosage Band for Inhaled Sarin

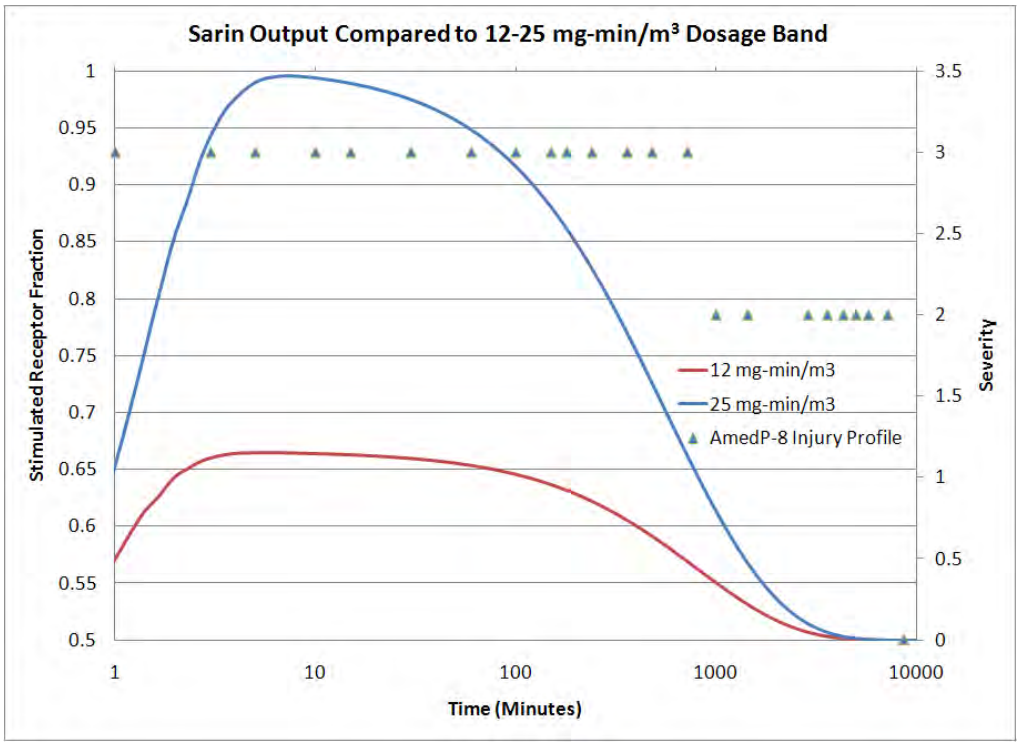

Figure 6-10. Model Results Compared to AMedP-8(C) 12 - 25 mg-min/m^3 Dosage Band for Inhaled Sarin

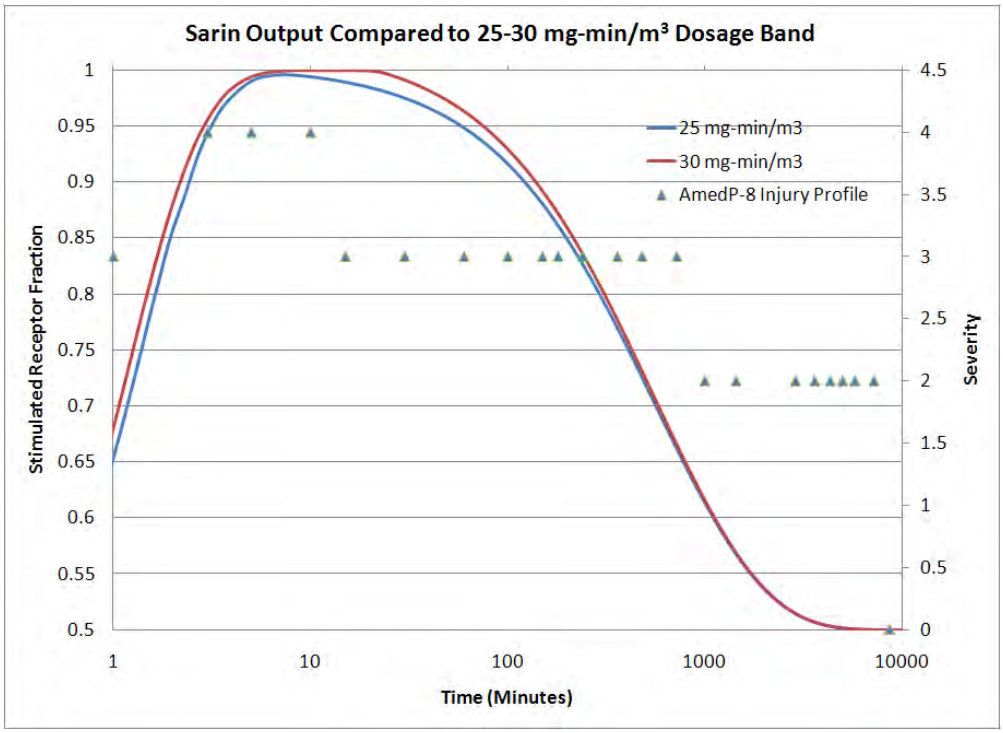

Figure 6-11. Model Results Compared to AMedP-8(C) 25 - 30 mg-min/m^3 Dosage Band for Inhaled Sarin

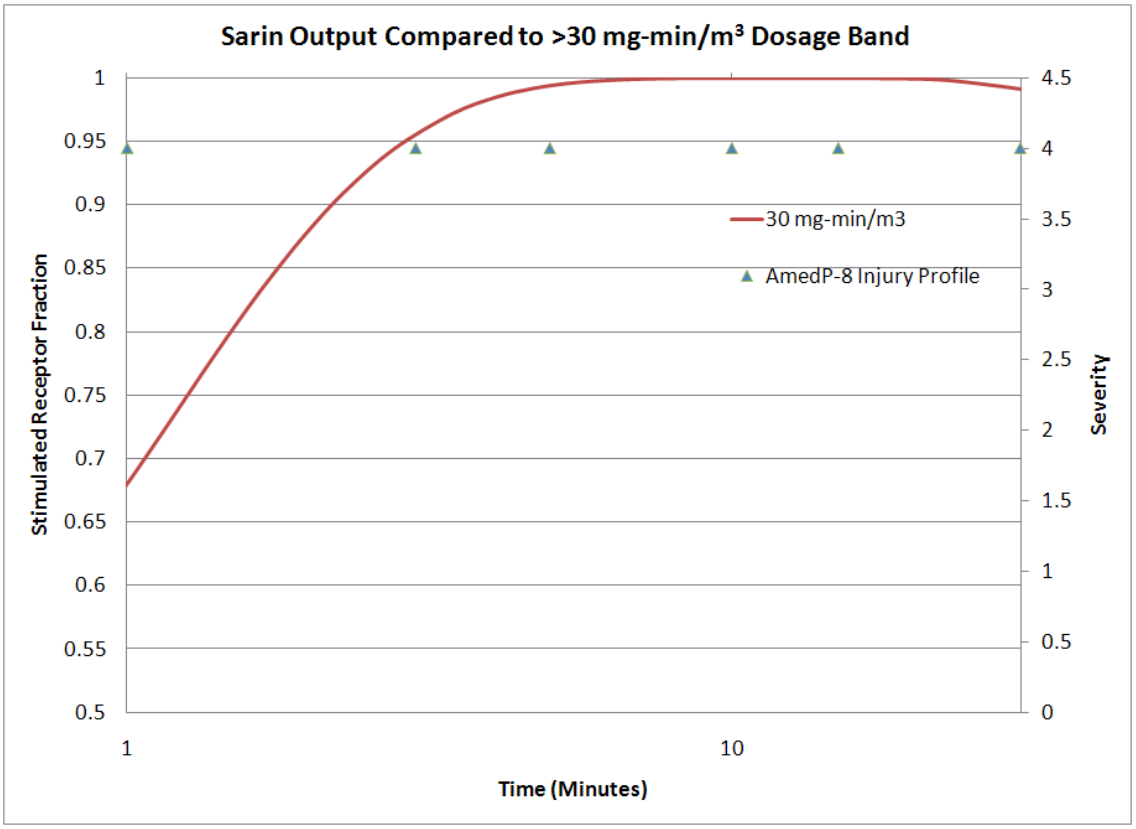

Figure 6-12. Model Results Compared to AMedP-8(C) > 30 mg-min/m^3 Dosage Band for Inhaled Sarin

As shown in the preceding figures, the model results for stimulated receptor fraction (in the absence of countermeasures) directly correlates to the symptom severity profiles from AMedP-8(C). Figure 6-7, which shows threshold effects for a sarin exposure, has stimulated receptor estimates that range from 50% (baseline) to 51% (very minor injury). In fact, AMedP-8 predicts nothing but mild ocular effects, so whole blood stimulated receptor fractions probably don't accurately capture the injury at these low dosages, as the major effect will likely be from percutaneous vapor exposure. Also of note is the recovery time in the model and how the stimulated receptor fraction begins to decrease as the severity of illness decreases. This trend holds for everything except for the higher doses. At the higher doses, the recovery (in terms of stimulated receptor fraction) happens at a faster rate than the AMedP-8 injury profiles suggest. But this is likely due to the fact that at these high dosages, the body has suffered a level of damage potentially requiring repair beyond acetylcholinesterase repair. What this suggests is that further extrapolation of the injury model will be required in order to map stimulated receptor fraction to sign/symptom severity. However, since countermeasures would no longer be effective at the times where divergence begins to occur (>1000 minutes), this level of modeling is out of scope for this particular effort.

6.3.2. Percutaneous VX Comparison

Comparing the model output for percutaneous VX exposure to the AMedP-8 sign/symptom severity estimates for VX is a bit more difficult than doing the GB/inhalation comparison. With

the AMedP-8 VX model, one has to take a VX exposure and assume it is an instantaneous exposure. However, percutaneous exposure is a prolonged exposure and, in the case of the percutaneous model being used for this effort, results in a maximum blood concentration of VX at 210 minutes post-exposure and a tapering off to trace levels at approximately 2000 minutes. It would be impossible to take that exposure and estimate an equivalent 10 minute exposure. We tried to shift the AMedP-8(C) injury profiles by 210 minutes as shown in Figure 6-13, and although the timing of sign/symptom progression looks as if it is better matched with AChE %, it is clear that the lowest AMedP-8(C) dosage band is producing values for the AChE % that are much lower than seen for sarin (which was above 90% available receptors for all doses within that band). However, looking at the higher end of the VX band (1.6 mg), we notice that it is higher than the FM 3-11.9 estimate of the LD_{10} for severe effects. Since our model is strongly tied to probability of lethality and effect, comparing the percutaneous model to the AMedP-8(C) percutaneous model is not recommended for this effort.

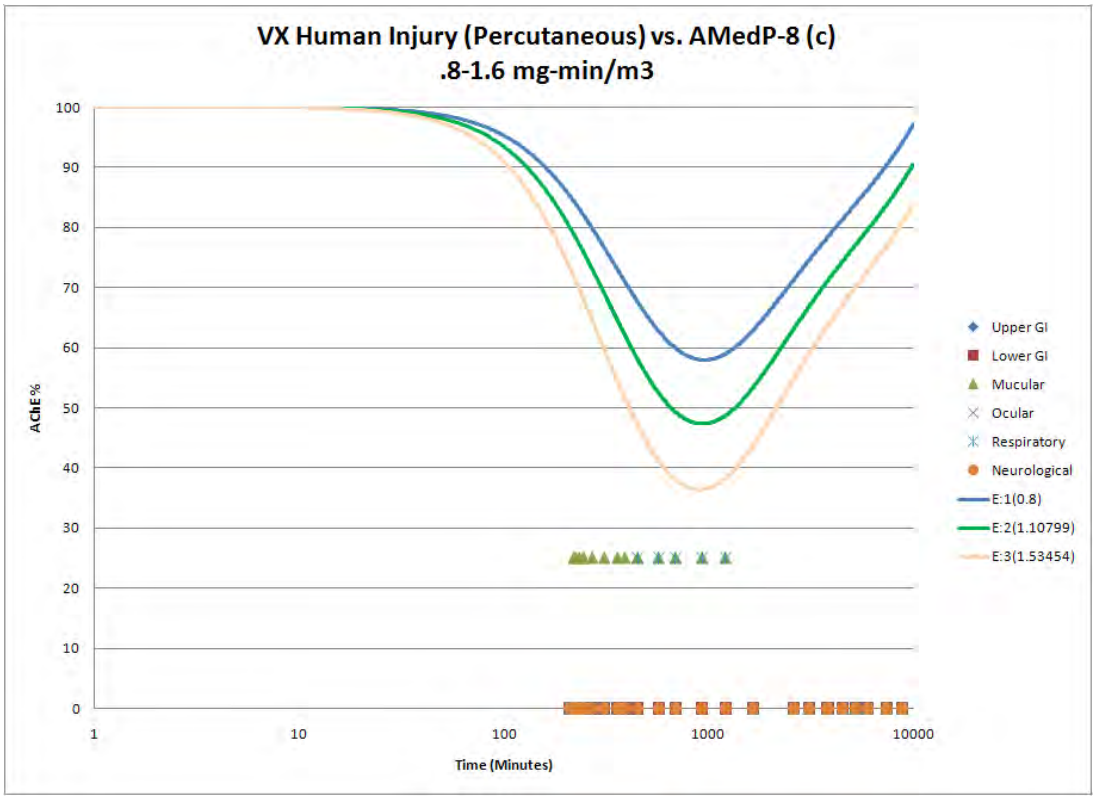

Figure 6-13. Model Results Compared to AMedP-8(C) 0.8-1.6 mg Dosage Band for Percutaneous VX

6.4 Model Application

One of the beneficial uses of the model is to study the impact of delayed treatment on probability of mortality. The ideal treatment for a soldier in the field that was exposed to a 2-minute LCt_{50} (33 mg-min/m^3) would be to use all three MARK I kits (for a total of 1750 mg of 2-PAM, 1400 mg of atropine, one minute post-exposure, and 70 mg of diazepam at the onset of seizures). With this treatment regimen, the probability of mortality decreases from 50% to 15%.

However, if the wounded individual only manages to use a single MARK I kit, the probability of mortality becomes 31%. If this same individual is given a second dose of 2-PAM at 60 minutes and a third dose at 120 minutes, the probability of mortality decreases to 23%. Figure 6-14 shows the stimulated receptor fractions for these three scenarios.

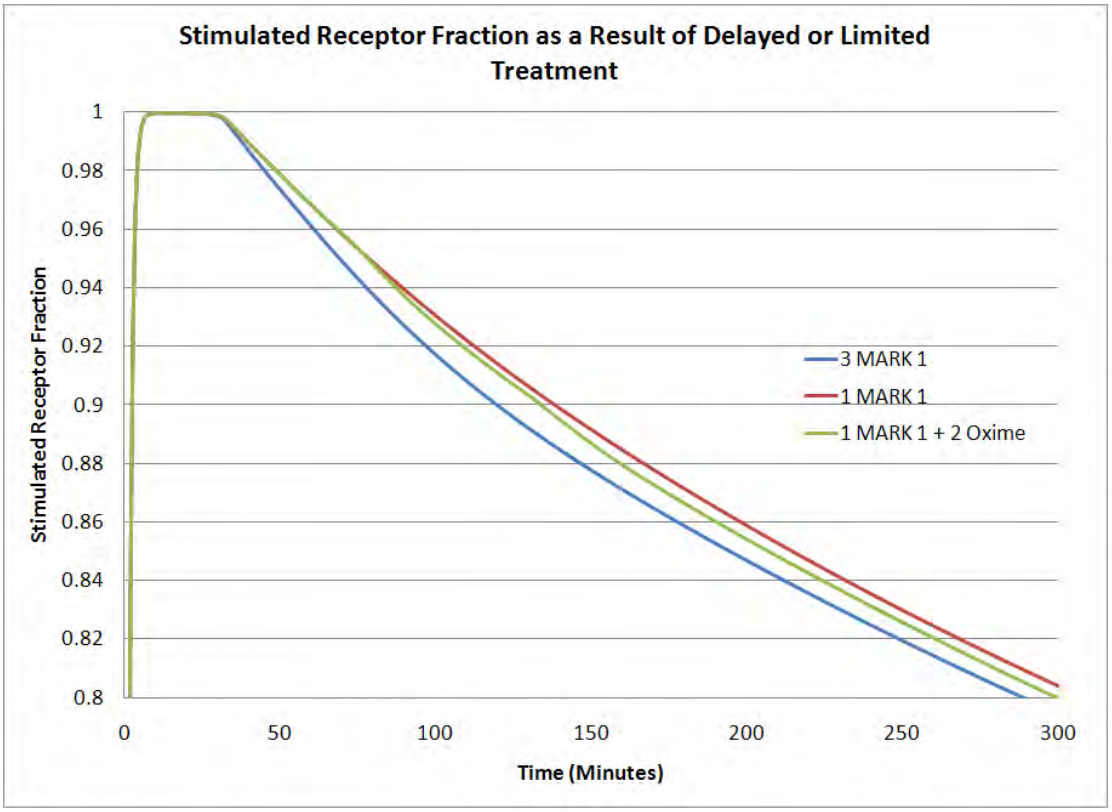

Figure 6-14. Stimulated Receptor Fraction as a Result of Delayed or Limited Treatment

As shown, giving the individual the equivalent of three MARK 1 kits one minute following exposure (blue) leads to a more rapid decrease in the stimulated receptor fraction. The scenario where the individual is given 2 additional doses of oxime (green), results in a slight decrease in the stimulated receptor fraction. This makes intuitive sense. For the three MARK 1 kit scenario, the 2-PAM reactivates more AChE than the one MARK 1 kit scenario starting at 3 minutes. Although there are still a lot of receptors being stimulated, there is more AChE available to cleave the ACh from the stimulated receptors. As these receptors are freed up, the diazepam works to slow the release of Ach, so that the atropine can bind with the receptors. This lowers the number of stimulated receptors that the AChE needs to free, thus reducing the number of stimulated receptors at a greater rate. In turn, the value of T_{dev} is reduced enough to significantly lower the probability of mortality.

We can also study the impact of delayed treatment. Assume that an individual is given three doses of 2-PAM at varying times (1 minute, 30 minutes, 60 minutes, 90 minutes, or 120 minutes post-exposure). Figure 6-15 shows the model results for these scenarios. As shown, the dose at 1 minute results in a steeper drop for stimulated receptors as the AChE continues to be reactivated by the oxime. However, in all cases the dose of oxime is still being administered while the

stimulated receptor fraction is above 0.8- the level at which there is some danger of mortality. So, in all cases there is a reduction in the probability of mortality. The probability of mortality for each scenario is shown in Table 5-15.

Table 6-1. Probability of Mortality for Delayed Treatment with 2-PAM against an LCt_{50} Dose of GB

Treatment Time (Post Exposure)	1-Minute	30-Minutes	60-Minutes	90-Minutes	120-Minutes
Probability of Mortality	18%	19%	23%	28%	33%

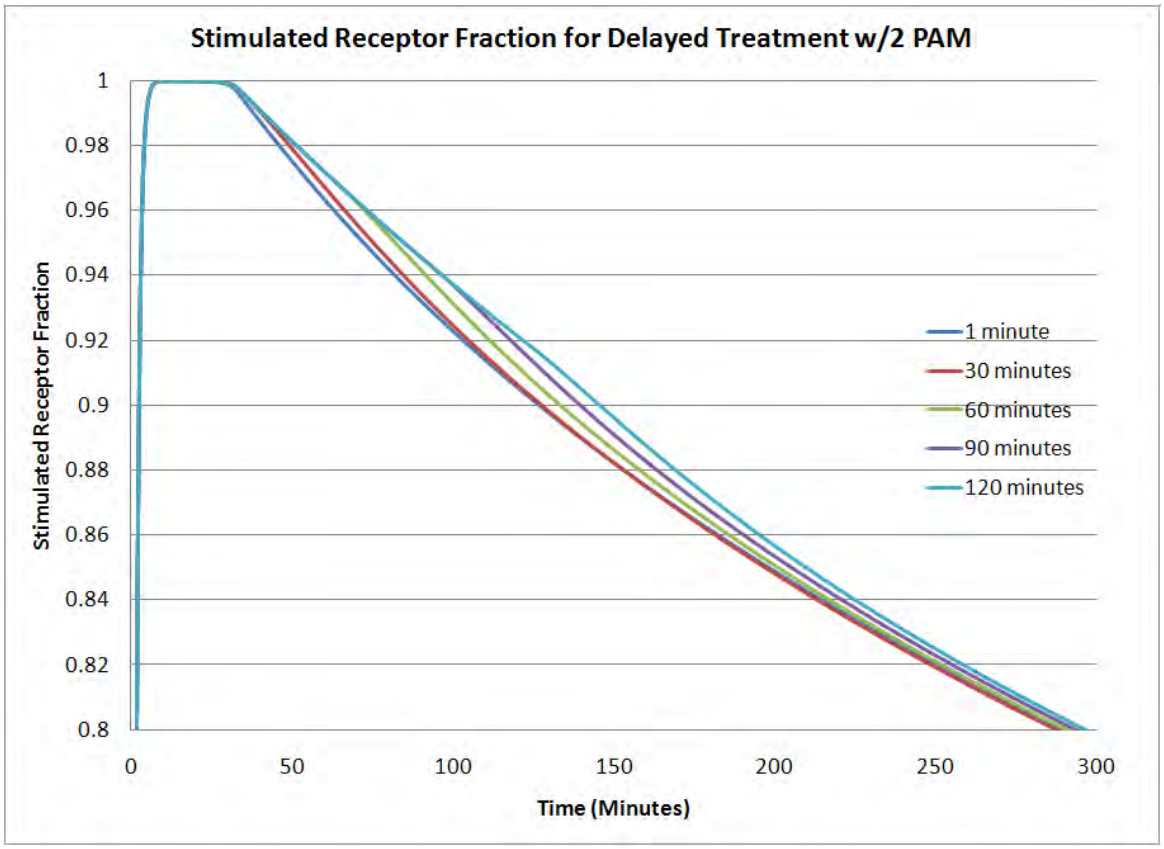

Figure 6-15. Stimulated Receptor Fraction for Delayed Treatment of 2-PAM against an LCT_{50} of Sarin

Variability in time of death was not included explicitly in this model of OP injury. As discussed earlier, T_{dev} is a time parameter proportional to the cumulative time spent under duress (high receptor stimulation), resulting in a probability of mortality. T_{dev} does not, however, represent an estimated time of death, which for an LCt_{50} of sarin, averages approximately a half hour in the AMedP-8(C) model. Table 6-2 shows the calculated T_{dev} values for the above treatment scenarios. Obviously, the oxime treatment must be administered before the time of death in order to lower the probability of mortality. Table 6-1 shows that the model predicts a reduction in mortality from 50% to 33% for an administration time of 120 minutes. This result

requires that the individuals representing the difference of 17% (about one-third of those who would die without treatment at the LCt_{50} dosage) have survived for two hours to receive the delayed treatment. In future work, we will further analyze the time of death issue and its relationship to the mortality model.

Table 6-2. T_{dev} for Delayed Treatment with 2-PAM against an LCt_{50} Dose of GB

Treatment Time (Post Exposure)	1 minute	30-Minutes	60-Minutes	90-Minutes	120-Minutes	No treatment
Probability of Mortality	27.0	27.1	28.0	28.8	29.4	31.0

The model can also be used to study the effectiveness of different oximes against a particular OP. Figure 6-16 shows the stimulated receptor fraction as a function of time for an LCt_{50} of GB with no treatment (blue), HI-6 (red), obidoxime (green), 2-PAM (purple), and MMB-4 (light blue). As the figure shows, obdoxime is the most efficacious against GB poisoning and 2-PAM is the least efficacious. The probabilities of mortality for the given oximes are given in Table 6-3.

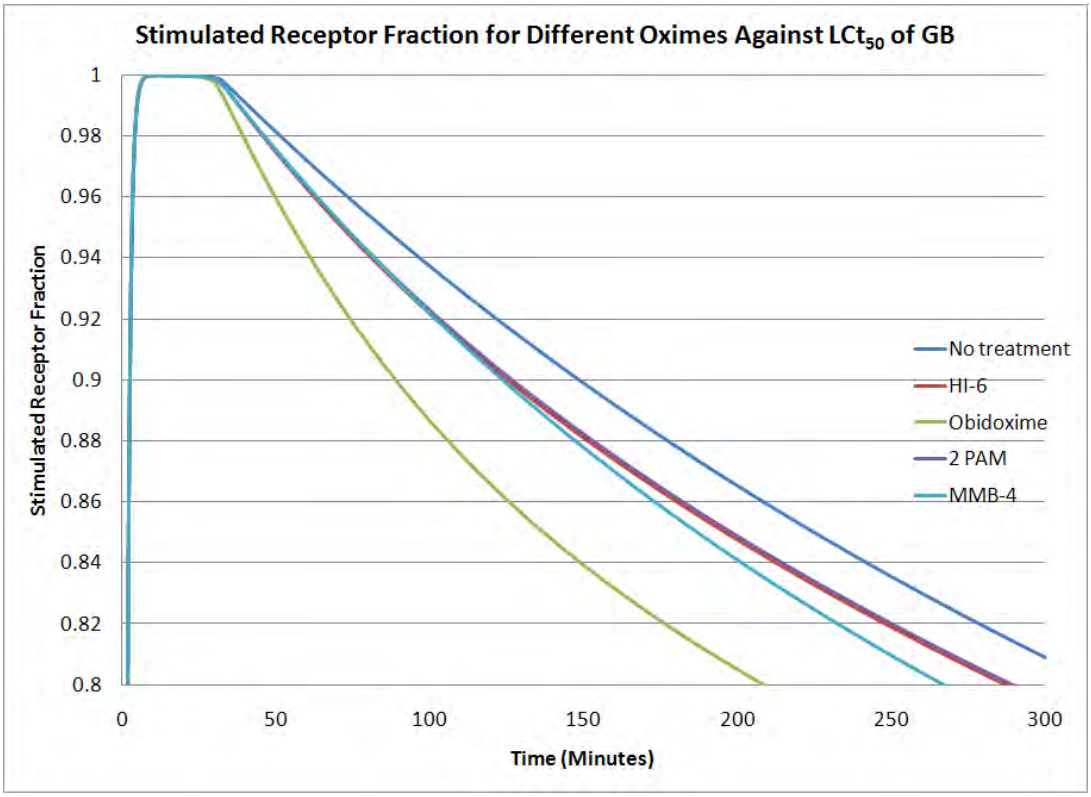

Figure 6-16. Stimulated Receptor Fraction for Different Oximes against an LCt_{50} of Sarin (Administered 1 Minute Post-Exposure)

Table 6-3. Probability of Mortality for Different Oximes against an LCt_{50} of Sarin (Administered 1 Minute Post-Exposure)

Treatment	No Treatment	HI-6	Obidoxime	2-PAM	MMB-4
Probability of Mortality	48%	17%	2%	18%	13%

Section 7.

Conclusions and Recommendations

The organophosphate injury and treatment/recovery model provides a novel model for studying the effects of OP on the body and efficacious effects of treatments. The injury model compares well to animal data, available human data, and the AMedP-8 injury profiles for inhaled agents. It also produces results consistent with the EPA's AEGL values, by accounting for biological repair and agent clearance for protracted exposures. The oxime model accounts for the reactivation of acetylcholinesterase in a way that is consistent with animal data and can be used to study the efficacy of oxime treatments for different doses, dosing frequencies, and oxime types. The atropine model accounts for the competitive binding at the receptor level, giving the oxime time to reactivate the acetylcholinesterase. The combined benefit of atropine and oxime was included in our model and has been verified by animal data. The diazepam model accounts for the depression of the central nervous system and the slowed release of acetylcholine, also giving the oxime time to reactivate the inhibited acetylcholinesterase. The bioscavenger model accounts for the sequestering of organophosphate in the blood, therefore raising the LD_{50} of the chemical agent.

There are limitations to the model. We believe that the model may be overestimating the beneficial effect of atropine, possibly by not accounting for the effect blocked receptors may have on the body. However, we believe that the overestimation is not significant but further investigation could be warranted. Also, we have no way of estimating the actual beneficial effects of bioscavengers in humans as they have not yet been used in human trials. With oximes, atropine, and diazepam we have seen beneficial effects with individuals that were accidently exposed to organophosphates. Whereas we can reasonably assume that bioscavengers would be beneficial, the data that is missing is the clearance rate for bioscavengers given to humans; we do not know how the effect of the bioscavengers will decrease over time.

Despite these limitations, we have developed a novel model that will greatly aid in the analysis of medical countermeasures against organophosphate exposure, allowing researchers and policy makers to reexamine requirements and treatment regimens, and estimate the effects of new countermeasures that fit into our model framework.

This page is intentionally left blank.

Section 8.

Works Cited

(NATO), N. A. (December 2007). *AMedP-8 (B), Volume I-III: Medical Planning Guide for the Estimation of NBC Battle Casualties.* STANAG 2475, 2476, 2477: North Atlantic Treaty Organization.

Aurbek, N., Thiermann, H., Szinicz, L., & Worek, F. (2007). Evaluation of HI 6 treatment after percutaneous VR exposure by use of a kinetic-based dynamic computer model. *Toxicology, 233*, 173-179.

Aurbek, N., Thiermann, H., Szinicz, L., Eyer, P., & Worek, F. (2006). Analysis of inhibition, reactivation and aging kinetics of highly toxic organophosphorus compounds with human and pig acetylcholinesterase. *Toxicology, 224*, 91-99.

Benschop, H. d. (2001). Toxicokinetics of Nerve Agents. In S. R. Somani, *Chemical Warfare Agents: Toxicity at Low Levels* (pp. 25-81). Boca Raton: CRC Press.

Biljana, A., & Stojiljkovic, M. P. (2007). Unequal Efficacy of Pyridinium Oximes in Acute Organophosphate Poisoning. *Clinical Medicine & Research, 5*(1), 71-82.

Cannard, K. (2006). The Acute Treatment of Nerve Agent Exposure. *Journal of the Neurological Sciences, 249*, 86-94.

Chugh, S., Aggarwal, N., Dabla, S., & Chhabra, B. (2005). Comparative Evaluation of "Atropine Alone" and "Atropine with Pralidoxime (PAM)" in the Management of Organophosphorus Poisoning. *JIACM, 6*(1), 33-37.

Clement, J., Bailey, D., Madill, H., Tran, L., & Spence, J. (1995). The acetylcholinesterase oxime reactivator HI-6 in man:pharmacokinetics and tolerability in combination with atropine. *Biopharm. Drug Dispos., 16*, 415-425.

Doctor, B. P., & Saxena, A. (2005). Bioscavengers for the Protection of Humans Against Organophosphate Toxicity. *Chemico-Biological Interactions, 157-158*, 167-171.

Doctor, B. P., & Saxena, A. (2005). Bioscavengers for the protection of humans against organophosphate toxicity. *Chemico-Biological Interactions*, 167-171.

Gearhart, J. M., Jepson, G. W., Clewell, H. J., Andersen, M. E., & Conolly, a. R. (1994). Physiologically Based Pharmacokinetic Model for the Inhibition of Acetylcholinesterase by Organophosphate Esters. *Environmental Health Perspectives, 102*(11).

Hörnchen, U., Schüttler, J., Stoeckel, H., Ensing, K., de Zeeuw, R., & Eichelkraut, W. (1989). Comparison of intravenous and endobronchial atropine: a pharmacokinetic and -dynamic study in pigs. *Eur J Anaesthesiol, 6*(2), 95-101.

J. van der Merwe, e. a. (2005, January). A Physiologically Based Pharmacokinetic Model of Organophosphate Dermal Absorption. *Toxicological Sciences, 89*, 188-204.

Jones, R., & Carrivick, L. (2010). *Percutaneous Exposure Model v1 Software Design.* Dstl/TR51815. Porton Down, Salisbury, Wiltshire: [dstl].

Joosen, M., & van der Schans, M. v. (2010). Percutaneous exposure to the nerve agent VX: Efficacy of combined atropine, obidoxime and diazepam treatment. *Chemico-Biological Interactions, 188*, 255-263.

Kassaa, J., Juna, D., Karasovaa, J., Bajgara, J., & Kucaa, K. (2008). A comparison of reactivating efficacy of newly developed oximes (K074, K075) and currently available oximes (obidoxime, HI-6) insoman, cyclosarin and tabun-poisoned rats. *Chemico-Biological Interactions, 175*, 425-427.

Koplovitz, I., Schulz, S., Raile, R., M. S., & Lee, R. (2007). Effect Of Atropine And Diazepam On The Efficacy Of Oxime Treatment Of Nerve Agent Intoxication. *J Med CBR Def, 5*.

Lanks, K. W., Dorwin, J. M., & Papirmeister, B. (1974). Increased Rate of Acetylcholinesterase Synthesis in Differentiating Neuroblastoma Cells. *The Journal of Cell Biology, 63*, 824-830.

Lenz, D. E., Yeung, D., Smith, J. R., & Sweeney, R. E. (2007). Stoichiometric and catalytic scavengers as protection against nerve agent toxicity: A mini review. *Toxicology*, 31-39.

Lundy, P., Hansen, A., Hand, B., & Boulet, C. (1992). Comparison of several oximes against poisoning by soman, tabun and GF. *Toxicology, 72*, 99-105.

Lundy, P., Hill, I., Lecavalier, P., Hamilton, M., Vair, C., Davidson, C., et al. (2005). The pharmacokinetics and pharmacodynamics of two HI-6 salts in swine and efficacy in the treatment of GF and soman poisoning. *Toxicology, 208*, 399-409.

Narouzi, P. (2010). A Novel Acetylcholinesterase Biosensor Based on Chitosan-Gold Nanoparticles Film for Determination of Monocrotophos Using FFT Continuous Cyclic Voltammetry. *International Journal of Electrochemical Science.*, 1434-1446.

North Atlantic Treaty Organization (NATO). (February 2010). *AMedP-8 (C) NATO Planning Guide for the Estimation of CBRN Casualties: Ratification Draft 1*. North Atlantic Treaty Organization: STANAG 2475.

Raveh, L., Grunwald, J., Marcus, D., Papier, Y., Cohen, E., & Ashani, Y. (1993). Human butyrylcholinesterase as a general prophylactic antidote for nerve agent toxicity. *Biochem. Pharmacol.*, 2465-2474.

Shih, T.-M., Skovira, J. W., O'Donnell, J. C., & McDonough, J. H. (2010). In vivo reactivation by oximes of inhibited blood, brain and peripheral tissue cholinesterase activity following exposure to nerve agents in guinea pigs. *Chemico-Biological Interactions*.

Sidell, F., & Groff, W. (1972). Intramuscular and intravenous administration of small doses of 2-pyridinium aldoxime methochloride to man. *J. Pharm. Sci, 61*, 1765-1769.

Sidell, F., Groff, W., & Kaminskis, A. (1972). Toxogonin and pralidoxime: kinetic comparison after intravenous administration to man. *J. Pharm. Sci., 61*, 1765-1769.

Skovira, J. W., O'Donnell, J. C., Koplovitz, I., Kan, R. K., McDonough, J. H., & Shih, T.-M. (2010). Reactivation of brain acetylcholinesterase by monoisonitrosoacetone increases the therapeutic efficacy against nerve agents in guinea pigs. *Chemico-Biological Interactions*.

Spruit, H. L. (2000). Intravenous and inhalation toxicokinetics of sarin stereoisomers in atropinized guinea pigs. *Toxicol. Appl. Pharmacol., 169*, 249-254.

Thiermann, H., Eyer, F., Felgenhauer, N., Pfab, R., Zilker, T., Eyer, P., et al. (2010). Pharmacokinetics of obidoxime in patients poisoned with organophosphorus compounds. *Toxicology Letters, 197*, 236-242.

USAMRICD. (July 2000). *Medical Management of Chemical Casualties Handbook: Third Edition.* APG, MD: U.S. Army Medical Research Institute of Chemical Defense (USAMRICD).

Valiyaveettil, M., Alamneh, Y., Rezk, P., Biggemann, L., Perkins, M. W., Sciuto, A. M., et al. (2011). Protective efficacy of catalytic bioscavenger, paraoxonase 1 against sarin and soman exposure in guinea pigs. *Biochemical Pharmacology, 81*, 800-809.

van der Schans, M. L. (2003). Toxicokinetics of the nerve agent VX in anesthetized atropinized hairless guinea pigs and marmosets after intravenous and percutaneous administration. *Toxicol. Appl. Pharmacol., 191*, 48-62.

Wagner, S., Kufleitner, J., Zensi, A., Dadparvar, M., Wien, S., Bungert, J., et al. (2010). Nanoparticulate Transport of Oximes over an In Vitro Blood-Brain Barrier Model. *PLoS One, 12*, 5.

Weinbroum, A. A. (2004). Pathophysiological and clinical aspects of combat anticholinesterase poisoning. *British Medical Bulletin, 72*, 119-133.

Worek, F., Aurbek, N., Wetherall, J., Pearce, P., Mann, T., & Thiermann, H. (2008). Inhibition, reactivation and aging kinetics of highly toxic organophosphorus compounds: Pig versus minipig acetylcholinesterase. *Toxicology, 244*, 35-41.

Worek, F., Eyer, P., Szinicz, L., & Thiermann, H. (2007). Simulation of cholinesterase status at different scenarios of nerve agent exposure. *Toxicology*, 155-165.

Worek, F., Eyer, P., Szinicz, L., & Thiermann, H. (2007). Simulation of Cholinesterease Status at Different Scenarios of Nerve Agent Exposure. *Toxicology, 233*, 155-165.

Worek, F., Eyer, P., Szinicz, L., & Thiermann, H. (2007). Simulation of Cholinesterease Status at Different Scenarios of Nerve Agent Exposure. *Toxicology, 233*, 155-165.

Worek, F., Reiter, G., Eyer, P., & Szinicz, L. (2002). Reactivation kinetics of acetylcholinesterase from different species inhibited by highly toxic organophosphates. *Molecular Toxicology, 76*, 523-529.

Worek, F., Wille, T., Aurbek, N., & Eyer, P. T. (2010). Reactivation of organophosphate-inhibited human, Cynomolgus monkey, swine and guinea pig acetylcholinesterase by MMB-4: A modified kinetic approach. *Toxicology and Applied Pharmacology*.

Yanagisawa, N., Morita, H., & Nakajima, T. (2006). Sarin experiences in Japan: Acute toxicity and long-term effects. *Journal of the Neurological Sciences, 249*, 76-85.

This page is intentionally left blank.

Section 9.

Definitions, Acronyms, and Abbreviations

1xLD50	A dose that is 1.0 times the LD50
2-PAM	Pralidoxime
ACh	Acetylcholine
AChE	Acetylcholinesterase
AChE %	Acetylcholinesterase activity (may be either a fraction or %)
AMedP-8	Allied Medical Publication 8
ARA	Applied Research Associates, Inc.
CB	Chemical and Biological
CBD	Chemical and Biological Defense
CNS	Central Nervous System
DoD	Department of Defense
dstl	Defense Science and Technology Laboratory (in the UK)
DTRA	Defense Threat Reduction Agency
GA	Tabun
GB	Sarin
GD	Soman
GF	Cyclosarin
Gryphon	Gryphon Scientific, LLC
HuBChE	Human serum butylcholinersterase
JPEO-CBD	Joint Program Executive Office for Chemical/Biological Defense
JPM-IS	Joint Program Manager-Information Systems
JSTO	Joint Science and Technology Office
LD50	Median lethal dose
LDX	Dose causing X% mortality
mAChR	Muscarinic Receptor
MCM	Medical Countermeasure
OP	Organophosphate
PBPK/PD	Physiology based Pharmacokinetic/Pharmacodynamic

RD	Research & Development
RD-CBI	Information Systems Capability Development Division
TBD	To Be Determined
UK	The United Kingdom of Great Britain
VR	Russian VX
VX	Nerve Agent VX

DEPARTMENT OF DEFENSE

DEFENSE THREAT REDUCTION
AGENCY
8725 JOHN J. KINGMAN ROAD
STOP 6201
FORT BELVOIR, VA 22060
ATTN: C. KILEY

DEFENSE TECHNICAL
INFORMATION CENTER
8725 JOHN J. KINGMAN ROAD,
SUITE 0944
FT. BELVOIR, VA 22060-6201
ATTN: DTIC/OCA

DEPARTMENT OF DEFENSE CONTRACTORS

QUANTERION SOLUTIONS, INC.
1680 TEXAS STREET, SE
KIRTLAND AFB, NM 87117-5669
ATTN: DTRIAC